Preprints.org

Review

Recent Progress in Flexible Microelectrode Arrays for Combined Electrophysiological and Electrochemical Sensing

Umisha Siwakoti , Steven A. Jones , Deepak Kumbhare , Xinyan Tracy Cui , Elisa Castagnola [*]

Review

Recent Progress in Flexible Microelectrode Arrays for Combined Electrophysiological and Electrochemical Sensing

Umisha Siwakoti [1], Steven A. Jones [1], Deepak Kumbhare [2], X. Tracy Cui [3,4,5] and Elisa Castagnola [1,3,6,*]

[1] Department of Biomedical Engineering, Louisiana Tech University; usi002@latech.edu

[2] Department of Neurosurgery, Louisiana State University Health Sciences, Shreveport

[3] Department of Bioengineering, University of Pittsburg

[4] Center for Neural Basis of Cognition, University of Pittsburgh

[5] McGowan Institute for Regenerative Medicine, University of Pittsburgh

[6] Institute for Micromanufacturing, Louisiana Tech University

* Correspondence: elisa@latech.edu

Abstract: Understanding brain function requires advanced neural probes to monitor electrical and chemical signaling across multiple timescales and brain regions. Microelectrode arrays (MEAs) are widely used to record neurophysiological activity across various depths and brain regions, providing single-unit resolution for extended periods. Recent advancements in flexible MEAs, built on micrometer-thick polymer substrates, have improved integration with brain tissue by mimicking the brain's soft nature, reducing mechanical trauma and inflammation. These flexible, subcellular-scale MEAs can record stable neural signals for months, making them ideal for long-term studies. In addition to electrical recording, MEAs have been functionalized for electrochemical neurotransmitter detection. Electroactive neurotransmitters, such as dopamine, serotonin, and adenosine, can be directly measured via electrochemical methods, particularly on carbon-based surfaces. For non-electroactive neurotransmitters like acetylcholine, glutamate, and γ-aminobutyric acid, alternative strategies, such as enzyme immobilization and aptamer-based recognition, are employed to generate electrochemical signals. This review highlights recent developments in flexible MEA fabrication and functionalization to achieve both electrochemical and electrophysiological recordings, minimizing sensor fowling and brain damage when implanted long-term. It covers multi-time scale neurotransmitter detection, development of conducting polymer and nanomaterial composite coatings to enhance sensitivity, incorporation of enzyme and aptamer-based recognition methods, and the integration of carbon electrodes on flexible MEAs. Finally, it summarizes strategies to acquire electrochemical and electrophysiological measurements from the same device.

Keywords: flexible MEAs; neurotransmitter detection; electrophysiology

1. Introduction

The development of a complete understanding of brain function remains one of the greatest challenges for both neuroscientists and neural engineers.

Neural communication involves both chemical and electrical signaling, with neurotransmitters operating on different timescales and interacting to regulate specific brain functions. Advancing our understanding of these intricate communication mechanisms requires multimodal implantable neural probes capable of concurrently monitoring electrophysiological signals and the multi-time-scale chemical dynamics (tonic and phasic) of multiple neurotransmitters across multiple brain locations, over extended time periods. By elucidating the interplay between electrical and

electrochemical signaling and their roles in both normal and pathological conditions [1–3], these devices could become instrumental in uncovering fundamental neuroscience principles and enabling therapeutic intervention for different neurological and psychiatric disorders [4–6].

Microelectrode arrays (MEAs) are widely used to record neurophysiological activity with single-neuron resolution across varying brain depths and widths, maintaining functionality over weeks to years [7]. However, stiff silicon-based MEAs implants create a "kill zone", characterized by reduced neuron density and increased glial encapsulation [8–10], which impairs electrophysiological and neurochemical measurements during chronic use [11–14]. Additionally, conventional MEAs typically incorporate metal microelectrodes (Au, Pt, Ir) that present poor sensitivity towards electroactive neurotransmitters, such as dopamine (DA), serotonin or 5-hydroxytryptamine (5-HT), and adenosine (AD).

In the past decade, significant efforts have been directed to tune the structural, functional, and dimensional properties of conductive and insulating components of these devices, with the aim of achieving appropriate chemical and electrical properties and matching the mechanical properties to those of the nervous system. Notably, micrometer-thick polymers, such as polyimide, parylene C, and SU-8, have been used as substrates for flexible MEAs to mimic the mechanical properties of soft brain tissue, thereby minimizing perpetual mechanical trauma and inflammation [15–17]. These flexible MEAs, along with subcellular scale features, have demonstrated seamless integration with neural tissue for stable, long-term recordings [16–21]. Furthermore, achieving high signal-to-noise-ratio, long-term electrical performance, and stable electrochemical detection necessitates the careful selection of conductive electrode materials. Various material coatings, such as iridium oxide [22–26], nano platinum [27–29], and conductive polymers [30–37], have been employed to reduce impedance and enhance the charge-transfer capability of metal-based MEAs. More recently, custom functionalization of flexible MEAs has enabled the electrochemical detection of both *electroactive and non-electroactive* neurotransmitters [30,38,39].

The inherent redox properties of electroactive neurotransmitters, including DA, 5-HT, AD, and melatonin (MT), allow them to be directly measured with electrochemical methods, preferentially at carbon surfaces [40–46]. In contrast, non-electroactive neurotransmitters, including acetylcholine (ACh), glutamate (GLU), and γ-aminobutyric acid (GABA), require alternative strategies for electrochemical detection [47–50]. These strategies include immobilization of target-specific enzymes on the microelectrode surface to catalyze reactions that generate electroactive byproducts, such as hydrogen peroxide (H_2O_2), which can then be detected electrochemically [47,50,51]. Additionally, aptamers – oligomers of artificial ssDNA, RNA, Xeno nucleic acid (XNA), or peptide designed to bind specifically to target molecules – can be immobilized on the microelectrode surface and engineered to undergo conformational changes upon target binding, generating electrochemical signals [39,47,52–54].

This review summarizes recent advancements in flexible MEA fabrication and functionalization to achieve: (1) multi-time scale (tonic and phasic) neurotransmitter detection, (2) flexible MEA functionalization strategies to combine electrophysiological and electrochemical sensing, including (a) composite coatings, and (b) incorporation of enzyme and aptamer, (3) integration of carbon electrodes on flexible MEAs, and (4) acquisition of electrochemical and electrophysiological measurements from a single device.

2. Tonic and Phasic Neurotransmitters Detection Using Flexible MEAs

The Materials Neurotransmitter release occurs over multiple timescales, including tonic and phasic release. Tonic release reflects the slower, continuous firing of neurons, which maintains the extracellular basal levels through extra synaptic diffusion (seconds to minutes [55,56]). Phasic release results from rapid burst-firing of neurons, leading to fast, high concentration burst in the synaptic cleft, (milliseconds to seconds), caused by neuronal firing in response to stimuli [55,57].

Fast Scan Cyclic Voltammetry (FSCV) at carbon fiber microelectrodes (CFEs) has been considered the gold standard for *in vivo* detection of electroactive neurotransmitters, significantly

advancing our understanding of their phasic dynamics [58–60]. A detailed description of FSCV has been provided in previous review papers [41,43,61,62]. A schematic of a typical FSCV waveform is presented in Figure 1A. FSCV relies on the direct electron transfer reaction between redox-active molecules and the carbon surface of the electrodes [41,43,62,63]. By sweeping a potential waveform at fast scan rates (400-1200 V/s), FSCV achieves a sub-second temporal resolution [64]. Different FSCV waveforms have been investigated for different analytes, including DA, 5-HT, AD, MT, guanosine (GN) and methionine-enkephalin (M-ENK), to identify the combination of holding/switching potentials and scan rate that maximizes sensitivity and minimizes fouling [41,46,65–71]. The waveform is scanned at a repetition frequency of 10 Hz (100-ms temporal resolution). Between scans, a holding potential is applied to the working electrode to selectively preconcentrate the target molecule on its surface [43,62,63,71,72]. While FSCV can measure phasic electroactive neurotransmitter release (rapid changes in concentrations), the necessity for background subtraction has prevented its use for tonic measurement [41,43]. Tonic neurotransmitter dynamics play a crucial role in modulating neural activity and behavior outcomes [64,73]. Moreover, alterations in the interaction between tonic and phasic neurotransmitter dynamics lead to abnormal neurological function and are implicated in multiple neurological disorders [56,74–78]. Therefore, MEAs capable of measuring both phasic and tonic neurotransmitter releases across multiple brain regions are essential for understanding brain function and dysfunction, advancing the diagnosis and treatment of these disorders.
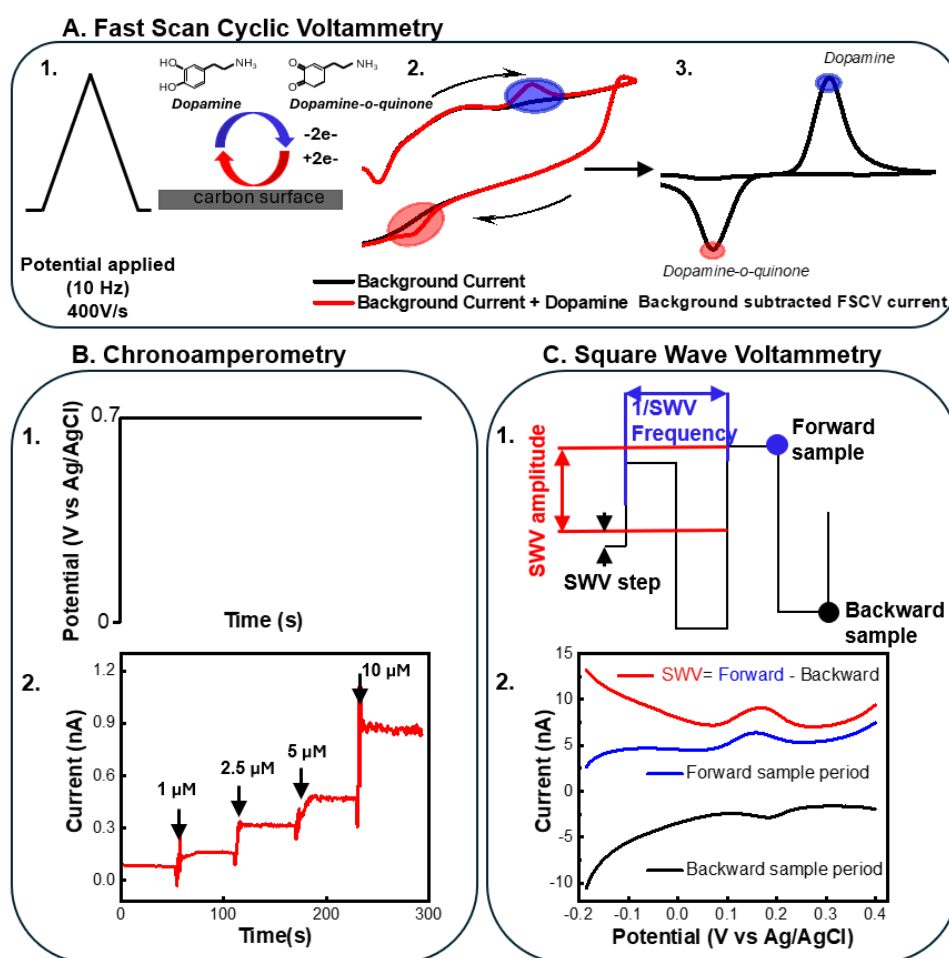

Figure 1. (A). Fast Scan Cyclic Voltammetry (FSCV); example of dopamine (DA) detection. After the application of a FSCV waveform from −0.4 to 1.3 V with scan rate of 400 V/s at 10 Hz at carbon microelectrode (1.), a background current is generated both in the presence (red) and absence (black) of 1 μM DA (2.). By subtracting the background signal, the DA oxidation and DA-o-quinone reduction peaks are isolated (3.). (B) Chronoamperometry; example of H2O2 detection. (1.) Waveform of amperometry at a voltage of +0.7 V (1.). (2.)

Current response of a nanoPt electrode to 1-10 µM of H2O2. (C) Square Wave Voltammetry (SWV) schematic. (1.) SWV waveform consists of a series of anodic and cathodic steps and holds that traverse a potential window defined by a stair step waveform. Forward current is measured at the end of each anodic hold period (blue marker) and backward current is measured at the end of each cathodic hold period (black marker) (2.). Representative SWV measurement of a 1 µM standard solution of DA at a PEDOT/CNT-coated GC microelectrode reveals a clear oxidation peak in the forward scan (blue) and a reduction peak in the backward scan (black). The final SWV current response manifests as a single current peak reflecting the difference between the forward and backward current responses (red).

Amperometry techniques, such as chronoamperometry and constant potential amperometry (CPA), if properly self-referenced [79], can measure phasic and tonic neurochemical events with high temporal resolution, enabling millisecond-scale continuous recording for hours without significantly interfering with electrophysiological signals [47,79–82]. An example of chronoamperometry waveform for H_2O_2 detection is presented in Figure 1B. However, its primary limitation is the lack of selectivity, as multiple electroactive species can contribute to the recorded current, complicating target identification. To tune selectivity, strategies such as modifying the applied potential to a value that is more sensitive to the desired analyte but less responsive to interferents, and/or applying selective membrane coatings are employed, minimizing interference and enhancing specificity [47,49,50,83,84]. Functionalized MEAs have been used for multi-channel amperometry detection of multiple neurotransmitters dynamics, both electroactive and not electroactive [49,85–88]. For example, ceramic MEAs, with Nafion coated-Pt electrodes, with or without m-phenylenediamine (m-PD), enabled tonic and phasic DA in rat striatum with CPA. This measurement was facilitated by a self-referencing amperometric method that subtracted signal from Nafion-coated electrodes and m-PD/Nafion-coated electrodes (sentinels) in real time[81]. Nafion acted as a selective barrier against negatively charged interferents, such as ascorbic acid (AA) and 3,4-dihydroxyphenylacetic acid (DOPAC), while m-PD served as a size exclusion filter, blocking larger molecules, including DA, from accessing the Pt recording sites [81].

Alternative electrochemical methods have been recently developed and optimized for tonic DA and 5-HT detection, including fast-scan controlled-adsorption voltammetry (FSCAV) [89–91], charge-balancing multiple waveform FSCV [92], convolution-based FSCV [93,94], fast cyclic square-wave voltammetry (SWV) [95,96], and N-shaped multiple cyclic SWV [97]. These techniques have been successfully applied *in vivo* and demonstrated successful detection of extracellular tonic DA concentrations in a ~50-100 nM range, and 5-HT concentrations in a ~60 nM range. However, these measures have been carried out at single CFEs, limited to a single active site per penetrating electrode [7,58,89–91,93–98]. Because neurotransmitter dynamics are complex and differ across various brain regions and even within subarea of the same region, high-resolution multisite measurements would be preferred [99–103].

Recently, SWV waveforms have been optimized to detect basal DA and 5-HT levels in rodent brains, both at poly(3,4-ethylenedioxythiophene) (PEDOT)/carbon nanotubes (CNT)-coated (PEDOT/CNT) and bare glassy carbon (GC) MEAs [38,104,105]. SWV is a pulse voltammetry technique in which a symmetrical square-wave pulse is superimposed on a staircase potential waveform. The current is sampled twice during each cycle: once at the end of the forward square-wave pulse and again at the end of the reverse pulse. The resulting signal is defined as the difference between the current measured during the forward and reverse pulses. SWV presents high sensitivity and effective isolation of faradaic currents—arising from redox reactions of electroactive analytes—from capacitive charging currents, thereby enabling precise detection of basal neurotransmitter levels [38,104,105]. The tonic DA and 5-HT concentration measurements obtained with SWV are comparable to those obtained with the previously mentioned voltammetric techniques [38,104,105]. A schematic of the SWV waveform is presented in Figure 1C.

Recently, the first implantable flexible MEA capable of multisite electrochemical sensing of both tonic and phasic DA dynamics *in vivo* has been demonstrated [38]. Phasic DA detection was obtained

with FSCV at GC microelectrodes. Tonic DA detection was measured using an optimized SWV waveform in combination with PEDOT/CNT coated microelectrodes [38]. More recently, miniaturized GC fiber-like (GCF) MEAs have been successfully used to measure tonic DA and 5-HT concentrations *in vivo* using SWV and stimulation-evoked phasic DA via FSCV. These devices also recorded neural activity in the striatum of mouse brains[104]. This novel design holds significant potential for multimodal measurements of neural activity and neurotransmitter concentrations, while maintaining an exceptionally minimal footprint (see section 3, Figure 5C).

3. Results Conductive Polymers and Composite Coatings for Electrophysiological Recording and Neurotransmitter Detection

This section may Conductive polymers, such as polypyrrole (PPy) and PEDOT, have gained considerable attention as neural electrode coatings due to their superior electrochemical performance and stability compared to metal electrodes [31–35,106–116]. Among many conducting polymers, PEDOT has shown superior chemical and electrochemical stability, making it the preferred choice for long-term *in vivo* applications[33,117]. The high surface area and ionic conductivity of PEDOT-based coatings drastically decrease the electrochemical impedance of metal electrodes, enabling high signal-to-noise ratio (SNR) recordings and enhanced charge injection capacity [33,35,36,109,118,119]. Thanks to its proven ability to improve recording performance, PEDOT:PSS has been used as a standard electrode coating for some of the most advanced flexible neural electrode designs, including the NeuroGrid [36], Neuralink[120], and NET devices [17].

Despite their superior electrochemical properties, such as low impedance and high charge transfer capability, when subjected to prolonged electrical stimulation during *in vivo* use, PEDOT-based coatings resulted in decreased charge injection limit, increased impedance, and delamination from the underlying substrate [26,121]. Different strategies have been investigated to improve PEDOT adhesion and long-term stability, with varying degrees of success. These strategies include substrate modification and functionalization [106,112,122–124], and the use of different dopants or co-dopants [107,122,125–128]. Comprehensive descriptions of these strategies are available in the review by Zheng et al. [122].

PEDOT-based composite coatings have also been extensively investigated for neurotransmitter detection [105,129–132]. PEDOT:nafion has been used to improve CFE sensitivity and fouling resistance in FSCV measurements. Electropolymerized PEDOT:Nafion significantly enhanced detection sensitivity for DA [131–133], 5-HT [133] and AD [133] compared to bare CFEs. Additionally, these coatings substantially reduced acute *in vivo* biofouling [131]. The incorporation of nanocarbon materials into PEDOT coatings, such as two-dimensional graphene oxide (GO) sheets [130] and acid-functionalized CNTs [38,105,129], has shown particular promise, not only in improving electrical stability and conductivity but also facilitating the absorption of monoamine neurotransmitters, thanks to the presence of functional groups.

PEDOT/graphene oxide (GO)-modified (PEDOT/GO) CFEs have been developed for enhanced DA detection using FSCV in rat dorsal striatum[130]. PEDOT/GO coatings have demonstrated an 880% increase in sensitivity and a 50% decrease in the limit of detection for DA compared to bare CFEs [130]. However, the thickness of these coatings must be carefully tuned to balance the increase in sensitivity without compromising adsorption or electron transfer kinetics. The enhanced DA sensitivity is attributed to the increased effective surface area and improved adsorption of DA's oxidation product (DA-o-quinone)[130].

Cui's group demonstrated that PEDOT/CNT-coated microelectrodes provide improved neural recording stability over four months compared to PEDOT:PSS recording sites [134], and exhibit excellent stability under electrical stimulation [126]. More recently, highly conductive PEDOT/CNT composite coatings have been incorporated into CFEs and optimized for highly sensitive and selective detection of resting DA levels in the rat striatum using SWV [129]. This electrochemical technique allows for direct measurement of tonic DA levels by selectively eliminating non-faradaic background charging currents. PEDOT/CNT functionalization significantly enhanced electrode

sensitivity for SWV-based DA detection, increasing sensitivity by 422-fold compared to bare CFEs [129]. Additionally, when selectively electropolymerized onto the metal recording site of silicon MEAs, these coatings enabled the first time-correlated, multi-site quantification of basal DA levels across different layers of the rat brain [129]. The same PEDOT/CNT coatings have recently been applied to flexible GC-MEAs [38,105]. When applied to bare GC microelectrodes, PEDOT/CNT increased DA sensitivity approximately sixfold using the previously optimized DA SWV waveform [38]. In a separate study, PEDOT/CNT-coated GC microelectrodes demonstrated 16 times higher sensitivity towards 5-HT than CFEs, even though the geometric area of the CFEs was seven times larger[105]. This enhanced sensitivity demonstrates the effectiveness of the optimized SWV waveform at PEDOT/CNT for detecting tonic 5-HT concentrations. Using this SWV waveform optimized for 5-HT, PEDOT/CNT-coated GC microelectrodes also show high 5-HT selectivity and fouling resistance [105]. The high sensitivity of the PEDOT/CNT-coated GC microelectrodes can be attributed to a much larger effective surface area of the PEDOT/CNT nanocomposite, as evidenced by reduced electrochemical impedance and increased charge transfer capabilities [38,105]. Furthermore, the incorporation of negatively charged functional groups on the surface of the electrode facilitates DA and 5-HT adsorption through electrostatic interactions, which have been shown to enhance their detection. Therefore, both the increased negative charge and the larger surface area contribute to enhanced sensitivity. These PEDOT/CNT-coated flexible GC-MEAs have enabled stable multisite *in vivo* detection of tonic DA for 21 days[38] and 5-HT for at least 7 days [105]. The chronic sensing stability may be attributed to several factors, including the high stability of the PEDOT/CNT coating on GC [38,105,107], the excellent electrochemical stability of both PEDOT/CNT [107,125,126] and GC [135,136], the high fouling resistance of negatively charged acid-functionalized CNTs [38,105,137,138], and the minimal glial inflammatory response induced by the flexible substrate [38,105].

Leveraging the excellent performance of PEDOT composite coatings for both electrophysiological recordings and electrochemical sensing, researchers have integrated PEDOT composite coatings into both stiff [139,140] and flexible [30,141,142] MEAs to enable dual measurement of both neurotransmitter concentrations and neural activity.

A single-wall carbon nanotube (SWCNTs)/PEDOT:PSS nanocomposite coating was applied to a 16 channel four-shank implantable silicon-based MEA to significantly enhance its electrical and electrochemical performance [139]. The improved electrical properties enable the MEA to detect electrophysiological signals with a high signal-to-noise ratio (SNR), while the enhanced electrochemical properties allow the MEA to respond sensitively and selectively to DA concentrations, using chronoamperometry at low oxidation potential (160 mV). The CNTs/PEDOT:PSS-modified MEA was used to acutely detect dual-mode signals, including electrophysiological activity and DA concentration, in the rat striatum under isoflurane anesthesia [139].

A composite of platinum black nanoparticles and PEDOT:PSS (PtNPs/PEDOT:PSS) was electrodeposited onto parylene C-based flexible MEAs to simultaneously measure spike firing and DA concentration [141]. DA detection was achieved using chronoamperometry at an oxidation potential of 0.35 V, with selectivity enhanced through the application of Nafion coating. These dual-mode flexible MEAs were utilized to monitor electrophysiological activity and dynamic changes in DA levels in the striatum of awake mice under fear-inducing conditions. The results revealed that after exposure to fear stimuli, decreases in the mean behavioral activity of the mice were accompanied by synchronous reductions in action potential firing rates, low-frequency (0–30 Hz) local field potential (LFP) power, and DA concentrations in the striatum. This study demonstrated the practicality of these flexible MEAs for the simultaneous detection of electrophysiology and DA dynamics [141].

PEDOT/CNT coatings were deposited on microfabricated flexible 20-channel polyimide MEAs for SWV-based dual-mode longitudinal detection of electrophysiological signals and tonic DA concentrations using SWV (Figure 2A,B). Similarly prepared PEDOT/CNT coatings have previously

demonstrated significantly enhanced electrode sensitivity for SWV-based DA and 5-HT detection compared to bare CFEs and GC-MEA microelectrodes [129], with high selectivity and fouling resistance [105]. The enhanced sensitivity of PEDOT/CNT-coated MEAs has been attributed to the larger effective surface area of the PEDOT/CNT. Additionally, the negatively charged functional groups on the acid-functionalized CNTs facilitate DA and 5-HT adsorption, further improving detection sensitivity [30,38,105].

The customized MEA channel layout (Figure 2 A) also enabled simultaneous monitoring of both cortical and striatal regions. These MEAs were adopted to investigate the involvement of DA dynamics in circadian rhythm regulation [30]. They were implanted in wild-type (WT) and Δ19 *Clock* mutant (MU) mice, which were hypothesized to exhibit changes in dopaminergic transmission, and recorded tonic DA concentrations and extracellular neural activity with high spatial and temporal resolution over four weeks. A diurnal fluctuation in DA concentration was observed in WT mice, but not in MU mice, which also exhibited higher basal DA concentrations and a stronger response to cocaine[30]. Additionally, the striatal neuronal firing rate was found to be positively correlated with DA concentration in both animal groups [30]. These measurements revealed that extracellular DA in the striatum is affected by the *Clock* gene.

Reduced graphene oxide (rGO)-doped PEDOT:PSS (rGO/PEDOT:PSS) coatings were electropolymerized into 128-channel ultrathin polyimide flexible MEAs to enhance DA sensitivity and electrical performance, enabling synchronous detection of electrical and electrochemical signals [142] (Figure 2 C-F). Similar to PEDOT/CNT, rGO/PEDOT:PSS coatings provided a large effective surface area rich in negatively charged functional groups, enhancing DA sensitivity [142]. DA levels were measured via constant potential amperometry at 0.2 V vs Ag/AgCl, ensuring stable voltage throughout the measurement with only brief crosstalk at the start and end of the recording. Given the presence of other electrochemically active substances in the body that can be oxidized at the same potential as DA, the electrode surface was coated with Nafion coating to enhance selectivity. These ultra-flexible devices (2.5 μm thick), with four shanks of 32 uniformly distributed microelectrodes, were implanted into the caudate putamen of the mouse brain, crossing multiple regions, including striatum, motor/primary sensory cortex and deep brain region simultaneously. The rGO/PEDOT:PSS-modified flexible MEAs reliably recorded local field potentials (LFPs), single-neuron activity, and DA fluctuations for over six weeks *in vivo*, while ensuring biocompatibility. These MEAs were used to observe and analyze the effects of nomifensine on both electrical and electrochemical brain activity, offering valuable insights into its *in vivo* mechanism of action and revealing the interplay and synergy between DA signaling and neural activity in different brain regions. Additionally, monitoring changes in the mice's trajectories allowed for the correlation of behavioral alterations with corresponding changes in brain activity [142].
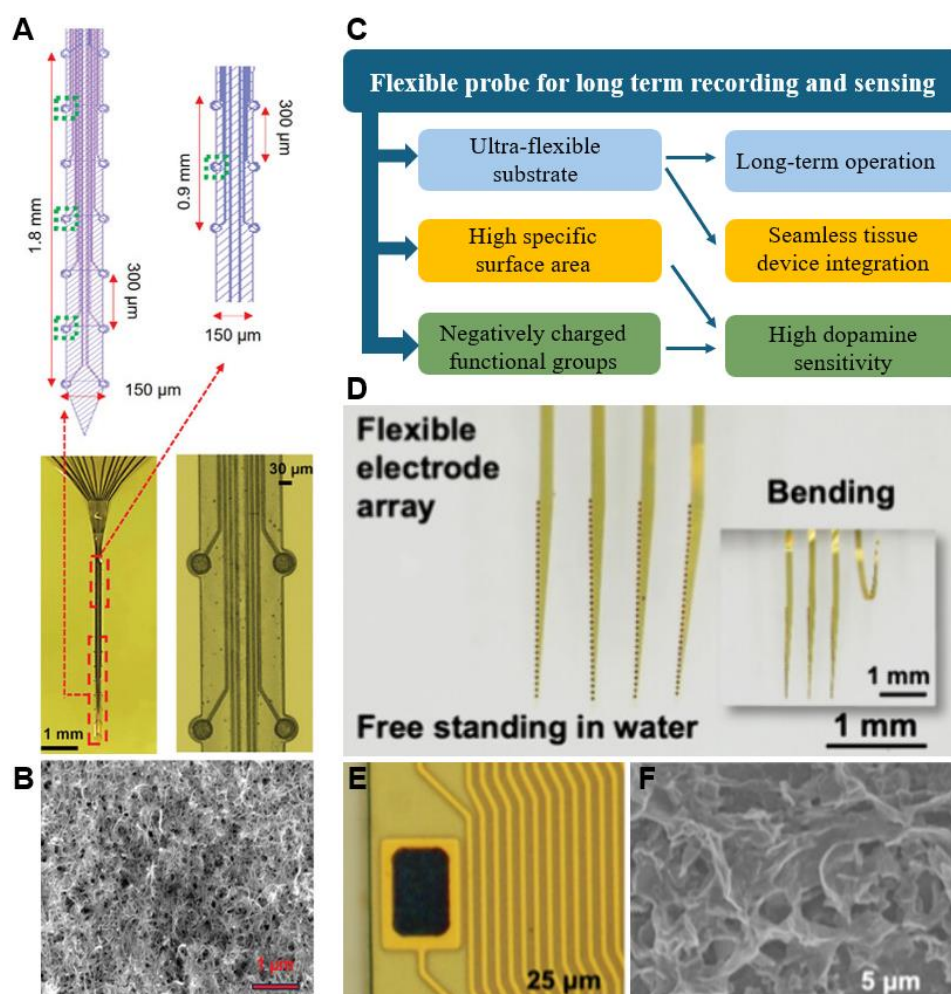
Figure 2. (A) MEA design layout (top), and optical images of the fabricated MEAs (below). The shank is 150 μm wide, 12 μm thick, and 5 mm long, with 300 μm spacing between individual sites. There are 20 channels in total, and the 4 sites in green boxes were only used for DA sensing. The optical image of the MEA shank: Region 1 (striatum) has 14 sites and region 2 (cortex) has 6 sites. The sites are 35 μm in diameter. Adapted from Wu et al. [30] (F) SEM image of PEDOT/CNT coating on top of Pt recording sites. Adapted from Wu et al. [30]. Copyright © 1999-2025 John Wiley & Sons, Inc. This publication is licensed under CC-BY 4.0. (C) Advantages of electrical and electrochemical performance of flexible rGO/PEDOT:PSS and PEDOT/CNT-modified electrodes. Adapted with permission from Wang et al. [142] (D) Optical image of released flexible electrode arrays (MEAs) in water. (E) Optical microscopic image of the modified electrode sites. Adapted with permission from Wang et al. [142] (F) SEM image of rGO/PEDOT:PSS coating. Adapted with permission from Wang et al. [142]. Copyright © 2024 American Chemical Society.

The chronic sensing stability of these flexible MEAs [30,142] may be attributed to several factors, including the good electrochemical stability of rGO/PEDOT:PSS [142] and PEDOT/CNT [30,107,125,126], the high fouling resistance of negatively charged acid-functionalized nanocarbon materials [30,38,105,137,138], and the minimal glial inflammatory response induced by the flexible substrate [30,38,105].

The dual measurement capability and chronic reliability of these flexible MEAs coated with organic polymer composites, i.e. PEDOT/CNT and rGO/PEDOT:PSS, highlight their potential for long-term *in vivo* electrochemical and electrophysiological monitoring, thus offering a powerful tool for advancing the understanding of brain function and driving breakthroughs in a wide range of neuroscience research areas (Figure 2 C).

4. Enzymatic and Aptamer-Based Detection

Authors Another type of electrochemical detection utilizes the immobilization of biological recognition elements onto the microelectrode's surface [47–50]. Typical recognition elements include target-specific enzymes or aptamers that interact with the target NTs to generate a measurable electrochemical response, enabling sensitive detection [39,47,49,50,84–87,143–147].

NT-specific enzymes immobilized on the microelectrode sites convert non-electroactive NTs into electroactive byproducts, such as hydrogen peroxide (H_2O_2), which can be detected using standard electrochemical methods, usually chronoamperometry [49,50,85–87,143–147]. NT-specific enzymes have also been used to detect electroactive NTs from metal microelectrodes [81,148,149].Representative schematic representation of the mechanism of Pt and nanoPt GLU sensor is provided in Figure 3A.

Electrochemical detection of ACh, GLU and GABA from ceramic MEAs has been established [79,81,85,87,143,144,150]. The MEA Pt electrodes have also been functionalize for multianalyte detection on the same device, including GLU and GABA [49,51,144], GLU and ACh [87], DA and GLU [88,140], choline (Ch) and ACh [86], Ch, GLU, glucose and lactate [151]. Pt electrodes are often preferred for their desirable catalytic effect on the oxidation of H_2O_2. An enzyme/crosslinker layer is typically deposited on the single recording sites of the array by manual drop casting. Size-exclusion screening layers are applied to reduce the influences of interfering molecules [49–51]. An enzyme-free 'sentinel' electrode on the array is used as a reference to subtract the background H_2O_2 signal.

Silicon-based MEA technology has also been used to simultaneously detect neurotransmitters and electrophysiological signals *in vivo* [140,151–153]. Manual drop casting can limit the throughput and requires large electrode size (15 × 333 μm [85,87] 50 × 150 μm [150]) not compatible with single-unit recordings. Crosslinking may also negatively affect the electrode impedance for electrophysiology measurements. High-surface-area coating, such as platinum nanoparticles (PtNPs) and reduced graphene oxide nanocomposites (Pt/rGO), have been used to lower the impedance of recording sites and increase sensitivity of sensing sites, additionally functionalized with enzyme/crosslinker layer [140,152]. MEAs modified with these coatings demonstrated the ability to dynamically record changes of neurotransmitters and neurophysiology activity in the hippocampus sub-regions of epileptic anesthetized rats [152], and awake mice [140]. Different electrodes of the same MEA were dedicated to electrical recording or chronoamperometry neurotransmitter detection, but the dual modal recordings were obtained simultaneously. These MEAs revealed that seizures in epileptic mice strongly correlate with changes in GLU, DA, and neuronal activity, which occurred before visible behavioral symptoms. The synchronized signal changes in the pre-seizure phase suggest the potential for early seizure prediction. This technology offers a valuable tool for studying epilepsy mechanisms [140].

However, chronic sensing over days and weeks *in vivo* has been challenging, possibly due to enzyme instability and/or foreign body reactions [154–156]. While flexible substrates can seamlessly integrate with the neural tissue [16,17,105], porous electrode materials are highly beneficial for enzyme immobilization [157–159]. Porous structures increase the effective surface area, enabling higher enzyme anchoring, minimizing the risk of detachment and protecting them from biological degradation. However, few attempts have been reported to combine these strategies in MEAs for electrochemical sensing.

Although ultra-flexible MEAs demonstrate stable neural recording, the success of these devices for long-term electrochemical sensing *in vivo* needs further investigation. Host tissue responses such as protein fouling, inflammatory cell attachment, and scarring exert additional challenges to analyte detection because biofouling interferes with electrochemical detection [138,160,161]. Additionally, tissue damage around the electrode hinders neurotransmitter diffusion to the electrode surface, distorting measurements [72]. A new flexible sensing MEA has been developed and functionalized for multi-site monitoring of spinal GLU signaling during myocardial ischemia and reperfusion in a large-animal model [50]. GluOx was crosslinked with bovine serum albumin (BSA) and glutaraldehyde on 3 of the 6 Pt electrode sites of the MEA (140 μm wide and ~16 μm thick, 6 × 100-μm-diameter electrodes), while the remaining 3 were used as sentinel sites. An m-Phenylenediamine

(mPD) film served as a size-exclusion screening layer to prevent electroactive species other than H_2O_2 from reaching the Pt electrode [50].

Probe flexibility offers significant advantages in terms of their capabilities to move with the neural tissue during micromotion that might be caused by cardiac pulsation or respiration [50]. Unlike stiff probes, the flexible design minimizes tissue damage and electrode breakage caused by large movement displacements. It also reduces motion artifacts, ensuring more reliable and robust recordings without causing significant trauma in the neural tissue. This is the first report of a flexible GLU sensor used in a large-animal model, highlighting the flexible probe's potential to advance neural monitoring in preclinical disease models [50].

In a subsequent study, a multichannel nanoPt GLU sensor similarly constructed on flexible Pt MEA (Figure 3A–E). The flexible MEAs were custom microfabricated to have electrode sites that are 200 μm apart to avoid crosstalk between channels and, when drop casting the enzyme coating, great care was taken to ensure that the coating did not extend past the electrode site onto the shank [49]. The modification of   platinum microelectrodes with nanometer-scale roughness (nanoPt) provides an effective method to significantly increase sensitivity and extend the stability of enzyme sensor to 3 weeks [49]. The additional surface area provided by the nanoPt offers additional anchor points to secure the enzyme (GluOx) to the surface, preventing enzyme loss over time. Furthermore, the increased surface area enhances the oxidation of H_2O_2 produced during enzymatic reactions, leading to higher electrode sensitivity (Figure 3D). *In vivo* stability tests in rodent brains showed that nanoPt GLU sensors remained functional for up to 7 days, whereas smooth sites on the same array failed by day 3. Additionally, increasing the effective surface area without increasing the geometric area allows electrodes to maintain a smaller footprint without compromising signal intensity, enabling the fabrication of higher-density MEAs with a small cross-section [49].

This flexible nanoPt GLU sensor MEA was successfully used to monitor GLU concentration changes induced by traumatic brain injury (TBI) in   rat model (Figure 3E–H)[49]. Inserted into the striatum with the aid of a sharpened tungsten wire, the MEA recorded baseline GLU for 10 minutes before TBI was generated using an impactor (Figure 3F). The impact caused a sustained 20-fold rise in GLU concentrations, consistent with TBI-related changes [49]. This was the first report of continuous GLU sensing throughout the cortical impact injury process from the same animal, enabled by the ultra-flexibility of the MEA thin film polymer substrate, which accommodates tissue displacement during impact. In the same study, similarly prepared flexible nanoPt sensor MEAs were successfully used to simultaneously sense GABA and GLU in the pig spinal cord [49] (Figure 3A–C,E, I,J).

These studies highlight the transformative potential of flexible and ultra-flexible MEAs in minimizing tissue damage, maintaining sensor functionality, and overcoming challenges such as tissue displacement and motion artifacts in electrochemical sensing.
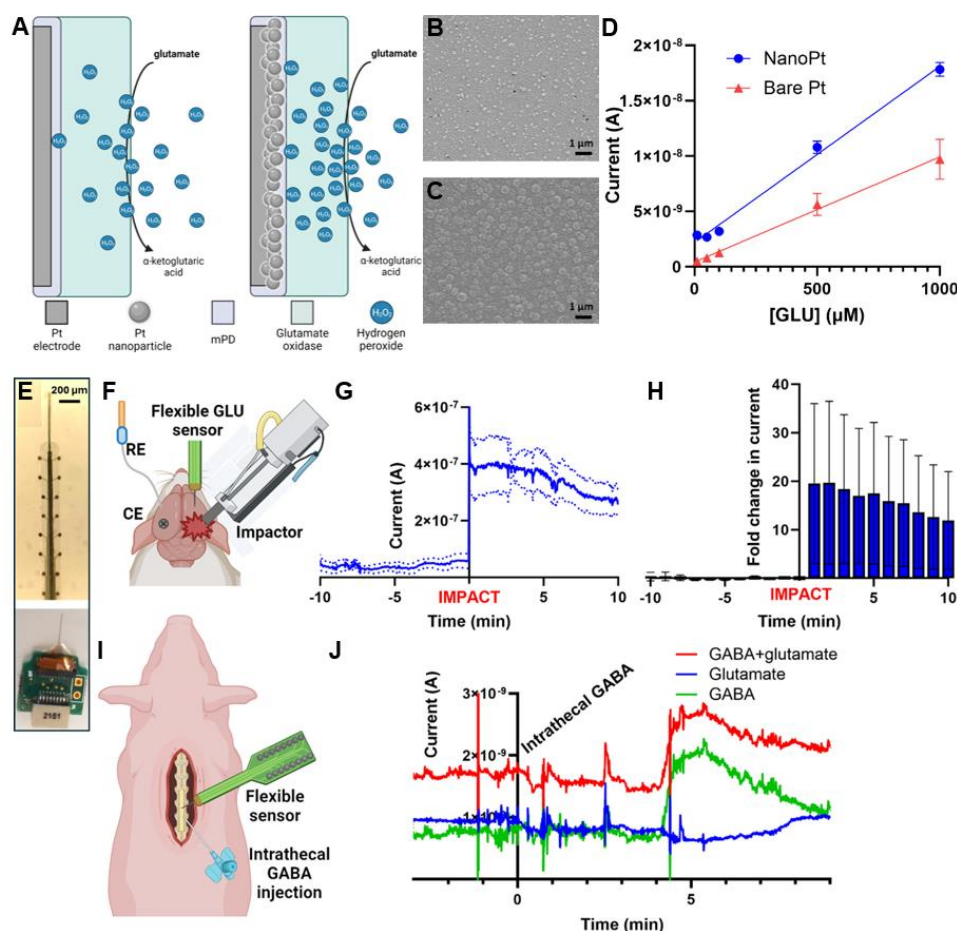
Figure 3. (A) Schematic representation of the mechanism of Pt and nanoPt GLU sensor. (B, C) Scanning electron microscope (SEM) picture of smooth Pt (B) and porous NanoPt (C). (D) GLU sensitivity of nanoPt sensors (blue) compared to smooth Pt sensors (red). (E) Optical picture of an assembled flexible MEA with a sharpened tungsten wire (top) and of the MEA inserted the ZIF connector of the custom PCB (bottom). (F) Schematic representation of the setup for recording GLU concentrations during traumatic brain injury (TBI). (G) The stable GLU baseline increased dramatically after the cortical tissue was damaged by the impactor. (H) For 10 min post impact, GLU signals remained elevated over 10-fold above baseline. (I) Schematic representation of the experimental procedure for measuring GLU and GABA in the porcine thoracic spinal cord. A flexible MEA functionalized for GLU and GABA sensing was inserted into the thoracic spinal cord. GABA was injected near the implantation site. (J) Simultaneous detection of GLU and GABA in the pig spinal cord. At t = 0 min, GABA is injected through a catheter into the spinal cord a few mm away from the sensor. Adapted from [49]. Copyright © 2024 The Authors. Published by American Chemical Society.   This publication is licensed under CC-BY 4.0.

Alternatively, aptamers - ssDNA, RNA, XNA strands artificially synthesized and selected to have high binding affinity to target molecules – can be immobilized on the microelectrode surface [39,47,52–54].
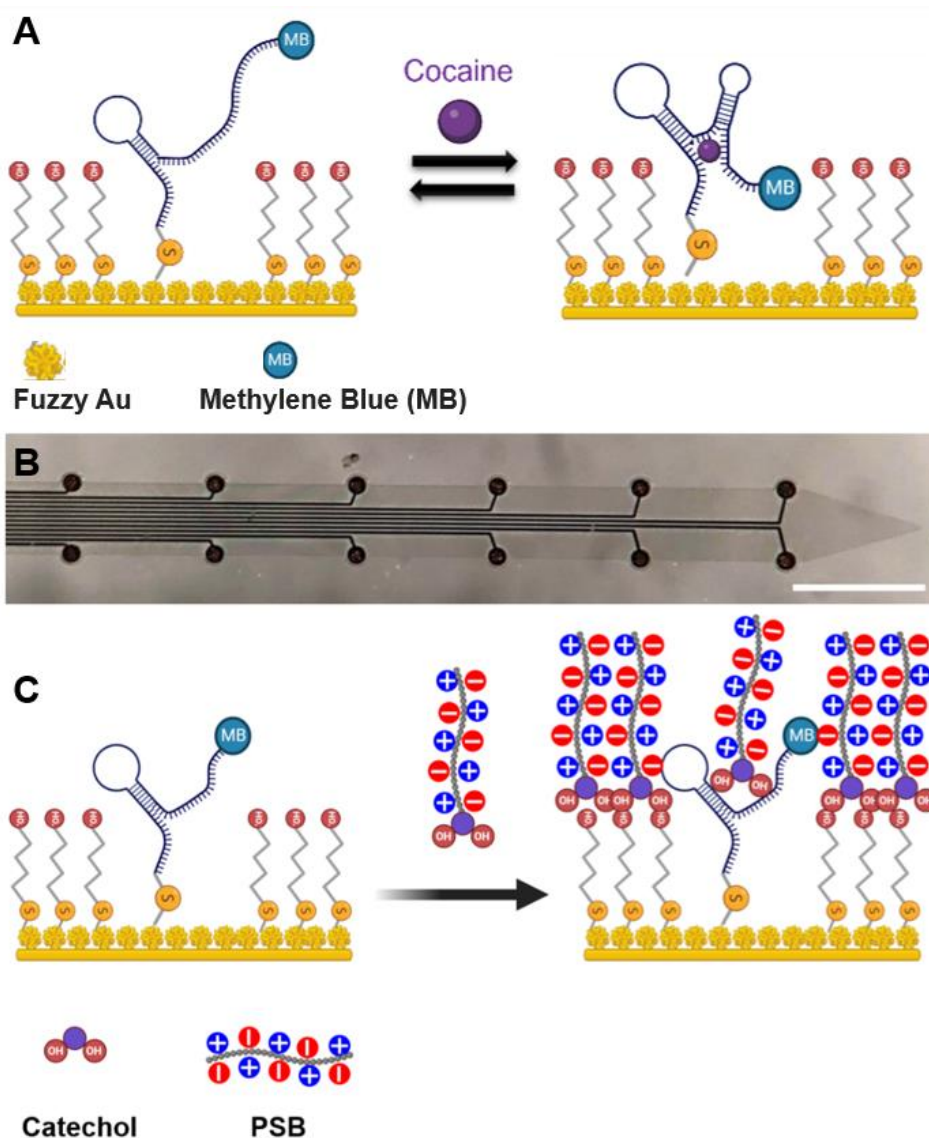
Figure 4. (A) Schematic demonstration of the standard self-assembly process for aptasensors and their detection mechanism. Fuzzy Au was first electrodeposited on electrode sites. Aptamers were then immobilized on the fuzzy Au surface. An additional self-assemble monolayer of 6-mercapto-1-hexanol (MCH) was immobilized as the passivation layer. Upon binding of the cocaine, the conformation change of aptamer brings the methylene blue (MB) tag closer to the surface, resulting in higher current response. **(B)** Flexible SU-8 thin film MEA for in vivo studies. 12 Au sites (35 μm diameter) with a spacing of 300 μm are distributed along both edges of the shank. Scale bar 300 μm. **(C).** Schematic demonstration of zwitterionic poly(sulfobetaine methacrylate) (PSB) deposition on standard cocaine aptasensors. The fabricated standard cocaine aptasensors were immersed in 10 mM tris buffer containing 2 mg/mL of PSB polymer for 2 h for coating deposition. The PSB polymers were anchored to the hydroxyl groups on the sensor surface through their catechol functional groups. Adapted from [39]. Copyright © 2023 by the authors. Licensee MDPI, Basel, Switzerland. This article is an open access article distributed under the terms and conditions of the Creative Commons Attribution (CC BY) license.

Affinity binding of target molecules to aptamers causes reversible conformational changes of the aptamers and entraps the molecule within the aptamers' chain. The reversible affinity binding of targets ensures that the target molecule is not consumed or absorbed in the process [162]. Electrochemical aptamer-based sensors have emerged as a promising approach for biomolecule detection [162,163]. In electrochemical aptasensors, aptamers are either employed in combination with field-effect transistors (FETs) to detect changes in surface charge [164–168] or functionalized with electrochemical reporter molecules, such as methylene blue (MB), ferrocene, or anthraquinone,

allowing direct detection of analyte binding through electrochemical techniques [39,169–173]. A wide range of aptamers have been developed for different target molecules, including cocaine [39,173,174], ATP [175–177], DA [148,178,179], and 5-HT [180–182]. However, only a few aptamer-functionalized MEAs have been successful for *in vivo* biochemical sensing [173]. The incorporation of cocaine aptamers into implantable silicon MEAs enabled effective cocaine detection and electrophysiological recordings in rat brains. However, the sensor's signal degraded within 1 hour of implantation [173]. Histological analysis identified a layer of biological material, including plasma proteins and microglial cells, forming on the electrode sites, potentially impairing the sensor's performance. To minimize undesired brain tissue responses and enhance stability in *in vivo* applications, an aptasensor was constructed on a flexible MEA with an SU-8 substrate [39]. Beyond mechanical considerations, surface chemistry plays a crucial role in the initial interactions between the device and host tissue. Since 90% of tissue is water, a promising antifouling approach involves coating the surface with a nanometer-thick layer of a zwitterionic polymer, creating a super-hydrophilic interface. This hydration layer effectively prevented protein adsorption and cell attachment [183,184]. Consequently, zwitterionic poly(sulfobetaine methacrylate) (PSB) coatings were applied as a non-fouling protective layer on these flexible aptamer-based MEA sensors to protect the implanted sensors from biofouling and to protect aptamers from enzymatic degradation in the extracellular environment. The efficacy of the PSB coating in maintaining sensor stability was evaluated both *in vitro* and *in vivo[39]*. The PSB coating protected the sensors from albumin fouling and DNase-1 enzyme degradation. *In vivo* studies demonstrated that PSB-coated MEA aptasensors could detect repeated cocaine infusions in the brain for up to 3 hours post-implantation without any loss in sensitivity [39]. Furthermore, the same MEAs could record electrophysiological signals from different tissue depths simultaneously. This innovative flexible MEA, integrated with cocaine sensors, provides a valuable tool for studying the mechanisms of cocaine addiction. Additionally, the PSB coating technology offers a generalizable solution to enhance the performance of implantable devices by mitigating biofouling and inflammatory host responses [39].

5. Integration of Carbon Material in Flexible MEAs

This Carbon is considered the ideal material for electrochemical detection of electroactive neurotransmitters due to its biocompatibility, sensitivity, capacitive electrochemical behavior, wide potential electrochemical window, fast electron transfer kinetics for neurochemical redox reactions, and excellent electrochemical stability [40,41,43,136,137,185–189]. Carbon fiber microelectrodes (CFEs) are considered the gold standard for measuring rapid neurotransmitter changes due to their small size (5 – 10 µm), biocompatibility, flexibility, and favorable electrochemical properties. However, traditionally assembled CFEs are typically limited to a single electrode site and manually encased in borosilicate glass [130,190–192]. These configurations are inserted into the brain using micromanipulators and guide cannulas, which can cause substantial tissue damage, posing challenges for chronic studies [191,192]. Recent advancements have introduced single CFEs [193,194] and CFE arrays [195–201] insulated with a poly(p-xylylene) or parylene thin-film coatings and designed as subcellular-scale probes for chronic implants. These configurations have enabled longitudinal measurements of sub-second evoked DA fluctuations over one year in rats [194] and for more than 100 days in non-human primates [202]. CFEs coated with conductive polymer coatings at the recording site have demonstrated stable results in chronic *in vivo* recordings, significantly reducing immune responses [193,203]. However, despite their promising capabilities, the fabrication of these electrodes remains highly manual and human-dependent, limiting scalability and feasibility for large-scale, batch production. Wafer-scale batch fabrication is crucial as it enables the simultaneous production of multiple devices with consistent quality and reproducibility that are essential for scaling up advanced technologies. Replacing metal with carbon in the wafer-scale batch fabrication of flexible MEAs, traditionally used for electrophysiological recordings, presents a transformative solution for integrating neurotransmitter detection capabilities. This innovation enables the realization of stable multimodal electrochemical and electrophysiological recordings by

leveraging the superior electrochemical properties of carbon materials alongside the enhanced biocompatibility of thin-film devices. However, only a few groups have successfully achieved batch fabrication of carbon-based MEAs on flexible substrates. The primary challenge is the high temperatures required for carbon synthesis, which are incompatible with polymeric substrates.   The solution to this challenge, the transfer of pre-patterned carbon structures from silicon wafers onto thin, flexible substrates, raises additional challenges [136,188,204,205].

An example of MEAs that use carbon microelectrodes on flexible substrates is a diamond-based microelectrode probe consisting of multichannel boron-doped polycrystalline diamond (BDD) microelectrodes integrated onto a soft Parylene C substrate[204] (Figure 5A). The fabrication process involved growing microcrystalline BDD films on wafers using microwave plasma-assisted chemical vapor deposition (MW-PACVD). These films were then patterned into microelectrodes using an aluminum mask in an electron cyclotron resonance reactive ion etcher (RIE). The pre-patterned BDD structures were subsequently transferred onto Parylene C films, with the growth side exposed as the sensing electrodes [204]. Morphological and electrochemical performance evaluations have demonstrated that electrodes fabricated from the BDD growth side exhibit superior characteristics compared to those made from the nucleation side. Specifically, the growth surface electrodes display a rougher morphology, higher sp^3 content, wider water electrochemical potential window, and faster dynamic kinetics. The nanoscale roughness and large grain size of the BDD microelectrodes increase their effective surface area, thereby reducing electrochemical impedance and minimizing noise during electrophysiological recordings, both *in vitro* and *in vivo[204]*. Additionally, electrodes fabricated from the BDD growth surface demonstrate improved *in vitro* DA sensitivity and a lower tendency for biofouling[204]. However, despite these advantages, diamond requires doping to achieve acceptable conductivity and does not achieve comparable sensitivity to smaller carbon electrodes, such as carbon CFEs [41,61] or GC [38,206].

Another example of MEAs with carbon microelectrodes on flexible substrates is the GC MEAs, which are obtained by integrating GC microelectrodes into flexible devices with metal interconnects, using a pattern transfer fabrication technique developed by Dr. Kassegne's lab [135,205,207]. GC microelectrodes are synthesized through the pyrolysis of a pre-patterned polymeric SU-8 precursor in an inert, controlled atmosphere. The possibility to photolithographically prepattern the SU-8 as a negative photoresist eliminates the need for post-patterning steps. The resulting GC microelectrodes are then transferred onto a flexible polymeric substrate [107,135,207,208]. The ability to precisely control the pyrolysis conditions plays a crucial role in achieving high-quality GC electrodes, which are essential for the sensitive and reliable performance of the GC MEAs. This technique has been successfully used to incorporate GC microelectrodes into 40 μm thick, polyimide-insulated implantable MEAs [206,208–210], which can penetrate brain tissue without external aid. These implantable MEAs, with GC microelectrodes and metal interconnections (hybrid GC-MEAs), demonstrated high sensitivity for FSCV detection of   DA and 5-HT *in vitro*, with good resistance to electrochemical fouling [206]. They also achieved high quality acute single-unit and local field potential recordings in rat [209] and songbird [208] cortices. When implanted in the songbird striatum, they enabled both *in vivo* detection of DA and high-quality single-unit recordings [210].
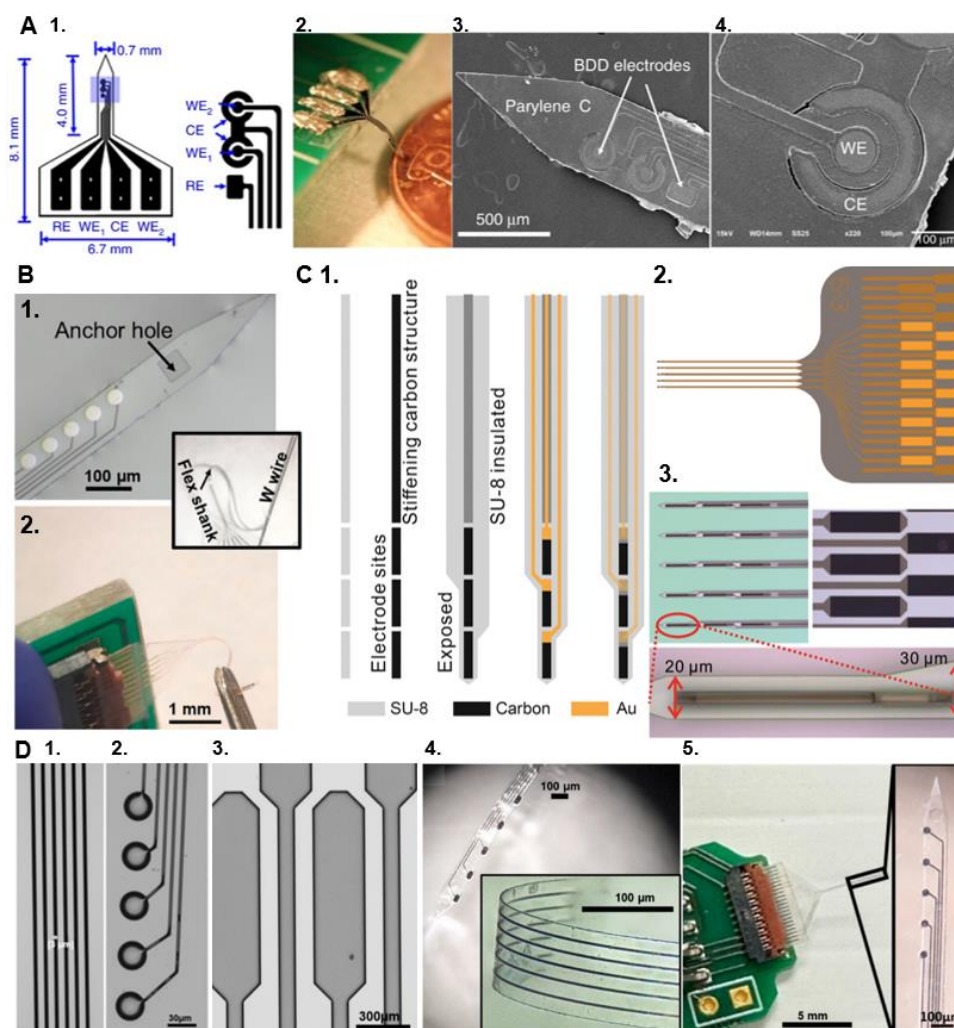
Figure 5. (A) Fabricated prototypes of a 2-channel electrode probe for electrochemical sensing and neural recording. (1.) The design of the implantable boron-doped polycrystalline diamond (BDD) probe, where the areas of the working electrodes (WE1/WE2), reference electrode (RE), and counter electrode (CE) are 0.0079, 0.028, and 0.035 mm2, respectively. (2,3) Photo and SEM images of a fabricated implantable neural probe. (4.) SEM close-up view of the BDD WE and CE. Adapted from Fan et al. [204]. Copyright © 2020, Springer Nature. Distributed under the terms of the Creative Commons CC BY. (B) Flexible GC-coated hybrid MEA. (1.) Optical picture of a GC MEA on SU-8 substrate with a metal interconnection and GC microelectrodes, after the release from the wafer. The inset shows a different view of the MEA flexible shank fabricated with an anchor hole at the shank tip to facilitate the insertion of a 50 µm tungsten shuttle that enables the handling and penetration of the probes into the brain. (2.) Flexible GC MEAs connected to the PCB using a zero-insertion force (ZIF) connector. Adapted from Castagnola et al. [38] Copyright © 2022 by the authors. Licensee MDPI, Basel, Switzerland. This article is an open access article distributed under the terms and conditions of the Creative Commons Attribution (CC BY) license. (C) Design and fabrication of GC fiber-like microelectrode arrays (GCF MEAs). 1) The fabrication process of the GCF. SU-8 is spin-coated and patterned on a wafer, followed by pyrolysis to produce carbon electrode sites and the stiffening structure. SU-8 is spin-coated and patterned to insulate the stiffening structure but exposing the electrode sites. Metal is patterned using lift-off procedures. The top layer of SU-8 is patterned to insulate the metal patterns. 2) The layout of the GCF array. 3) Optical microscopy images of the GCF array. Adapted from Castagnola et al. [104] Copyright © 1999-2025 John Wiley & Sons, Inc. Distributed under the terms of the CC BY 4.0. (D) Fabricated "all" GC-MEA with CG electrodes and interconnects. (1) Glassy carbon (GC) traces (2.) GC microelectrodes and (3.) GC pads on silicon substrate, prior to being transferred. (4.) finally insulated all GC-MEA (140 µm wide and ~8 µm thick, oval GC electrodes) during the peeling off from the PDMS (zoom of the folding in inset), and (5.) finally insulated all GC-MEA connected to the custom-made printed circuit board (PCB) using a zero-insertion force (ZIF) connector to be interfaced with the potentiostat for

characterization and sensing. The inset shows a magnification of the corresponding shank (120 μm wide and ~8 μm thick, 30 μm diameter circular GC electrodes). Adapted from Nimbalkar et al. [211]. Copyright © 2024 by the authors. Licensee MDPI, Basel, Switzerland. This article is an open access article distributed under the terms and conditions of the Creative Commons Attribution (CC BY) license.

Recent advancements have enabled the miniaturization of these hybrid GC-MEAs on thin, flexible SU-8 substrates (Figure 5B) [38,105]. These flexible GC-MEAs have achieved multisite electrochemical recordings of DA and 5-HT, and they exhibited reduced tissue damage and inflammation compared to stiff silicon probes, preserving a healthier neural tissue interface [105]. However, their flexibility necessitates a metal wire shuttle for penetration into deeper brain regions and they have a larger footprint than single CFE [38,105].

To enable self-insertion, the fabrication method has been adapted for batch production of GC fiber-like (GCF) MEAs [104] (Figure 5C). This novel design incorporates fiber-like GC structures on thin-film substrates, with an additional GC-fiber-like backbone that stiffens the MEAs for insertion but remains disconnected from the metal interconnections. The long, relatively stiff GCF structures, with an extremely small cross-section, allow the device to penetrate the brain tissue without aid. GCF MEAs also exhibit enhanced sensitivity toward DA and 5-HT compared to 7μm CFEs. GCF MEAs have been successfully used to measure tonic DA and 5-HT concentrations *in vivo* when combined with optimized SWV waveforms and to detect stimulation-evoked phasic DA via FSCV, from the same implanted device. They also recorded single-unit electrophysiological activity in the striatum of mouse brains. This novel design holds significant promise for multimodal measurements of neural activity and neurotransmitter concentrations while maintaining an exceptionally minimal footprint [104].

Another fabrication technique, named double-pattern transfer photolithographic process, has been developed for the fabrication of flexible polyimide GC-MEAs with GC electrodes and interconnects ("all" GC-MEAs),[136] to address potential concerns regarding the adhesion between metal interconnections and GC electrodes (hybrid GC-MEAs), which may not withstand prolonged and aggressive electrical or mechanical stresses in chronic applications. The first "all GC" prototype demonstrated exceptional performance, including *in vitro* FSCV DA detection and robust electrochemical stability during prolonged current delivery [136]. These results highlight their potential for creating stable neural interfaces. However, further miniaturization of these "all GC" design is required to achieve chronic electrochemical sensing applications. To advance this effort, Dr. Castagnola's lab recently published a proof-of-concept study on the fabrication of GC MEAs with GC electrode and interconnections on thin, flexible substrates with significantly reduced dimensions [211] (Figure 5D). The study explored the strengths and limitations of two microfabrication methods: (1) a double pattern-transfer photolithographic process, that transfer-bonds the MEAs on a temporary polymeric support, and (2) a double-etching process, that uses a 2 μm-thick low-stress low-pressure chemical vapor deposition (LPCVD) nitride (Si_3N_4) coating of the Si wafer as the bottom insulator layer for the MEAs, eliminating the need for pattern-transfer. Although both methods demonstrated feasibility, further optimization is needed to achieve the process control and scalability required for reliable batch fabrication, particularly for devices with miniaturized features [211].

An alternative approach to fabricate devices with carbon electrodes and interconnections is the laser-induced carbonization process on polymeric substrates. Laser-induced graphene (LIG) directly grown from commercially available polyimide (PI) or tailored PIs via laser irradiation, has gained attention for the synthesis of large-area, porous graphene materials with tunable pore density, ideal for advanced electrode designs [188,212–216]. This approach enables direct writing of graphene features on flexible substrates with facile patterning and high throughput production. The porous morphology, atomic structure and chemical composition of LIG are controllable by tuning the laser parameters such as laser power, raster speed, laser spot size, and spot overlap [212,217]. Additionally, molecular control of PI composition can be used effectively to tailor heteroatom compositions of the resulting LIG without the need for external doping sources [212].

A novel graphene-based neural interface, named "NeuroString", has been recently developed to seamlessly integrate with the central nervous system (CNS) and gastrointestinal (GI) tissue using a LIG method[218]. Transition metal nanoparticles, specifically 5,10,15,20-tetrakis-(4'-aminophenyl) iron (III) porphyrin chloride, and 5,10,15,20-tetrakis-(4'-aminophenyl) nickel (II) porphyrin, were incorporated into a polyamic acid polymer precursor to produce nanoparticle-modified graphene networks via a CO_2 LIG process [218]. The resulting nanoporous graphene network demonstrated exceptional electrochemical properties. Combined with the advantages of rapid laser patterning and an efficient transfer process enabled by the polystyrene block-poly(ethylene-ran-butylene)-block-polystyrene (SEBS) polymer as an insulator, this innovative platform enables the rapid fabrication of customized patterns. 3-channel NeuroString sensors (90×50 μm^2 in size) were temporarily rigidified using pullulan coating to assist the implantation in mouse brain, and they were successfully used for multi-channel FSCV detection of optically stimulated and behavioral DA dynamics in mouse the nucleus accumbens (NAc), and optically stimulated 5-HT response in the basolateral amygdala (BLA)[218]. Chronic implantation studies demonstrated that NeuroString provides reproducible DA signals for up to 16 weeks, along with enhanced biocompatibility and reduced tissue response compared to conventional rigid probes [218].

Although LIG technology offers numerous advantages, including rapid prototyping and material versatility, it is constrained by the resolution limits of the laser's spot size [219]. This limitation affects the fabrication of extremely fine features, particularly those smaller than 50-100 μm, which are essential for advanced miniaturized devices. The typical line widths achieved with LIG (50-100 μm)[218] are significantly larger than a single CFEs (7 μm)[129,190], or GC traces, which can be fabricated down to 3 μm [211].

While the integration of carbon materials into flexible, batch-fabricated devices has proven to enable reliable multimodal sensing, minimize tissue damage, and improve long-term stability, continued advancements in carbon microelectrode technologies, such as novel fabrication techniques and miniaturization, are essential to revolutionizing chronic neurochemical sensing and multimodal neural interface designs.

6. Acquiring Electrochemical and Electrophysiological Measurements from a Single Device

To comprehensively understand the dynamic interactions between chemical and electrical communication in neuronal circuits, integrated tools capable of simultaneously measuring chemical release (electrochemistry) and electrical activity (electrophysiology) within the central nervous system (CNS) are indispensable. To achieve dual measurement, it is essential to combine MEAs with multimodal capabilities with hardware designed to collect and integrate these datasets without electrical crosstalk. A detailed review of the various strategies used to achieve combined electrochemical and electrophysiological measures can be found elsewhere [79].

In summary, two main approaches have been used and are summarized below.

The *parallel approach* involves the use of separate microelectrodes dedicated to either electrochemical or electrophysiological acquisition. For example, different ceramic MEAs, with sites dedicated to either one or the other measurements, have been developed and used for multi-channel amperometry detection of neurotransmitters and electrophysiological (LFP/spike activity) electrophysiological acquisition [80,140,147,152,153,220,221]. The two datasets are collected from spatially separate sites. However, the inter-site distance is known, and inter-experiment variability is limited by the reproducibility of MEA manufacturing techniques. Using this approach, simultaneous multi-analyte detection and electrophysiological activity recording have also been recently achieved [88,140,151]. Chronoamperometry and constant potential amperometry measurements did not significantly impact neuronal activity *in vivo*, with only brief crosstalk occurring at the beginning and end of the recording. These transient electrical artifacts lasted for 3 to 5 ms [80,220].

The *serial or sequential approach*, uses a single microelectrode to measure both neurochemical releases, and single-unit neuronal activity by alternating between recording modes [222,223] . This

serial approach involves switch circuits that allow "time sharing" between recording modes, and has been used for detection of DA [223] and/or oxygen [224,225] by FSCV while recording single-unit neural activity at the same microelectrode in the interval between FSCV scans. This is possible thanks to the sub-second temporal resolutions of the FSCV that aligns with the timescale of chemical dynamics at neuronal synapses [226–230]. During these combined experiments, a triangular waveform is applied at 5 Hz, half the normal FSCV frequency. Every scan takes less than 10 ms and scans are repeated at 200 ms, to provide ~180 ms of electrophysiological recording between scans [231,232]. The advantage of this strategy is that both datasets are recorded at the same microelectrode, thus the same cell population/brain region is studied. Description of the hardware used for combined electrochemical and electrophysiological recordings in awake animals are summarized in [233,234]. This approach has only been done with one recording site at the time, but it can be extended to MEAs.

For the multimodal measurements described in this paper, involving SWV in combination with FSCV and/or electrophysiology, SWV measurements were performed sequentially on the same recording sites due to instrument limitations[30,38,104]. This sequential scanning introduced a temporal lag across different channels, requiring the sensing data to be averaged over 5-minute time bins, which underutilized the temporal resolution of the technique. A multichannel potentiostat system that can simultaneously scan all channels will eliminate this issue [30].

An alternative approach, fast sampling amperometry (FSA), has been recently investigated [79]. This approach utilizes high-frequency constant-potential amperometry for seamless single-sensor recordings of neurochemical and electrophysiological events. At a 40 Hz sampling rate, a 4-site MEA captured LFPs and electrochemical signals, linking acetylcholine release to hippocampal theta oscillations [235]. With higher sampling rates (100–1000 Hz), this method demonstrated concurrent recordings of metabolic and oxygen fluctuations with LFPs in rodent models [79,236]. This approach allows for real concurrent recordings in both the temporal and spatial domains, requiring a single instrument [79].

For all the approaches mentioned, a significant limitation lies in the limitations of hardware used to conduct multichannel simultaneous electrochemical measurements.

The novel MEA technologies enable the concurrent recording of neural electrical signals and neurotransmitter detection, providing a comprehensive platform to explore the complex interactions between electrical and chemical signaling in the brain. Designed with flexible polymers and functionalized surfaces, these MEAs have shown great promise in reducing mechanical trauma and inflammation, supporting stable, long-term multimodal neural recordings.

One key development is the use of nanomaterials, particularly nanocarbon-based conductive polymer composites, which enhance the electrochemical performance of the MEAs. These materials offer a larger surface area, low-impedance electrodes that improve the signal-to-noise ratio in electrophysiological recordings, and increased sensitivity and stability for extended neurotransmitter monitoring.

Another transformative development is the substitution of metals with carbon in the batch fabrication of flexible MEAs. This innovation improves both electrochemical performance and biocompatibility, facilitating stable, multimodal electrochemical and electrophysiological recordings through the advantageous properties of carbon materials.

Neurotransmitter-selective electrochemical detection, which relies on the immobilization of biological recognition elements such as enzymes or aptamers on the microelectrode's surface, has also been substantially improved through the use of nanoporous surfaces, flexible MEA substrates, and zwitterionic polymer encapsulation. However, enzyme and aptamer degradation in biological environments remain a challenge, and current immobilization methods present limitations. For example, manual drop-casting provides low throughput and can result in variable coating coverage and thickness. Crosslinking may also negatively affect the electrode impedance for electrophysiology. Improved immobilization techniques are needed to improve coating precision,

increase throughput, and enhance device stability and performance, particularly for long-term monitoring in complex biological environments.

As these MEA technologies continue to evolve, their application in understanding the complex interactions between electrical and chemical signaling in the brain will provide valuable insights into neurological disorders and the effects of therapeutic interventions. To fully realize the potential of these MEA devices for multimodal measurements, specialized hardware is needed to efficiently collect and integrate electrochemical and electrophysiological datasets without causing electrical interference.

The current approaches for multimodal acquisition are limited by either spatial or temporal resolution, as well as channel count, reducing both efficiency and precision in multimodal mapping of the brain. These constraints emphasize the need for improved hardware to enable high channel count, high-resolution, and simultaneous measurements. Advancements in miniaturization, data processing, and integration are essential to overcoming these challenges. Such improvements will allow for more effective management of complex datasets, expanding the utility of flexible MEAs in both research and clinical settings. Ultimately, these developments will lay the foundation for next-generation diagnostic tools and therapies, significantly advancing the field of neuroscience.

7. Conclusions

This review highlights recent advancements in flexible MEAs designed for both electrophysiological and electrochemical monitoring of neural activity. These developments include strategies to integrate neurotransmitter detection at multiple time scales (tonic and phasic), enable simultaneous detection of multiple analytes, and employ methods to minimize sensor fouling and brain damage for long-term performance.

The novel MEA technologies enable the concurrent recording of neural electrical signals and neurotransmitter detection, providing a comprehensive platform to explore the complex interactions between electrical and chemical signaling in the brain. Designed with flexible polymers and functionalized surfaces, these MEAs have shown great promise in reducing mechanical trauma and inflammation, supporting stable, long-term multimodal neural recordings.

One key development is the use of nanomaterials, particularly nanocarbon-based conductive polymer composites, which enhance the electrochemical performance of the MEAs. These materials offer a larger surface area, low-impedance electrodes that improve the signal-to-noise ratio in electrophysiological recordings, and increased sensitivity and stability for extended neurotransmitter monitoring.

Another transformative development is the substitution of metals with carbon in the batch fabrication of flexible MEAs. This innovation improves both electrochemical performance and biocompatibility, facilitating stable, multimodal electrochemical and electrophysiological recordings through the advantageous properties of carbon materials.

Neurotransmitter-selective electrochemical detection, which relies on the immobilization of biological recognition elements such as enzymes or aptamers on the microelectrode's surface, has also been substantially improved through the use of nanoporous surfaces, flexible MEA substrates, and zwitterionic polymer encapsulation. However, enzyme and aptamer degradation in biological environments remain a challenge, and current immobilization methods present limitations. For example, manual drop-casting provides low throughput and can result in variable coating coverage and thickness. Crosslinking may also negatively affect the electrode impedance for electrophysiology. Improved immobilization techniques are needed to improve coating precision, increase throughput, and enhance device stability and performance, particularly for long-term monitoring in complex biological environments.

As these MEA technologies continue to evolve, their application in understanding the complex interactions between electrical and chemical signaling in the brain will provide valuable insights into neurological disorders and the effects of therapeutic interventions. To fully realize the potential of these MEA devices for multimodal measurements, specialized hardware is needed to efficiently

collect and integrate electrochemical and electrophysiological datasets without causing electrical interference.

The current approaches for multimodal acquisition are limited by either spatial or temporal resolution, as well as channel count, reducing both efficiency and precision in multimodal mapping of the brain. These constraints emphasize the need for improved hardware to enable high channel count, high-resolution, and simultaneous measurements. Advancements in miniaturization, data processing, and integration are essential to overcoming these challenges. Such improvements will allow for more effective management of complex datasets, expanding the utility of flexible MEAs in both research and clinical settings. Ultimately, these developments will lay the foundation for next-generation diagnostic tools and therapies, significantly advancing the field of neuroscience.

Abbreviations

The following abbreviations are used in this manuscript:

MEAs	Microelectrode arrays
DA	Dopamine
5-HT	Serotonin
AD	Adenosine
ACh	Acetylcholine
MT	Melatonin
GLU	Glutamate
GABA	γ-aminobutyric acid
H2O2	Hydrogen Peroxide
XNA	Xeno Nucleic Acid
FSCV	Fast Scan Cyclic Voltammetry
SWV	Square Wave Voltammetry
CFEs	Carbon Fiber Microelectrodes
GN	Guanosine
M-ENK	Methionine-enkephalin
CPA	Constant potential amperometry
m-PD	m-phenylenediamine
AA	ascorbic acid
DOPAC	3,4-dihydroxyphenylacetic acid
CNT	carbon nanotubes
GC	Glassy carbon
FSCAV	fast-scan controlled-adsorption voltammetry
GCF	GC fiber-like
PPy	Polypyrrole
GO	graphene oxide
SWCNTs	single-wall carbon nanotube
NSR	Signal-to-noise-ratio
WT	wild type
MU	Δ19 Clock mutant
rGO	Reduced graphene oxide
PtNPs	platinum nanoparticles
nanoPt	Nano Platinum
TBI	traumatic brain injury
FETs	field-effect transistors
MB	methylene blue
PSB	poly(sulfobetaine methacrylate)

BDD	polycrystalline diamond
MW-PACVD	microwave plasma-assisted chemical vapor deposition
RIE	reactive ion etcher
LPCVD	low-stress low-pressure chemical vapor deposition
LIG	Laser-induced graphene
NAc	Nucleus Accumbens
BLA	Basolateral Amygdala
LFPs	Local Field Potentials
CNS	Central Nervous System
FSA	Fast Sampling Amperometry

References

1. A.E. Pereda, Electrical synapses and their functional interactions with chemical synapses, Nature Reviews Neuroscience 15(4) (2014) 250-263 https://doi.org/10.1038/nrn3708.
2. P. Alcami, A.E. Pereda, Beyond plasticity: the dynamic impact of electrical synapses on neural circuits, Nature Reviews Neuroscience 20(5) (2019) 253-271 https://doi.org/10.1038/s41583-019-0133-5.
3. A.C. Miller, L.H. Voelker, A.N. Shah, C.B. Moens, Neurobeachin is required postsynaptically for electrical and chemical synapse formation, Current Biology 25(1) (2015) 16-28 https://doi.org/10.1016/j.cub.2014.10.071.
4. T.N. Lerner, L. Ye, K. Deisseroth, Communication in neural circuits: tools, opportunities, and challenges, Cell 164(6) (2016) 1136-1150 https://doi.org/10.1016/j.cell.2016.02.027.
5. L.A. Jorgenson, W.T. Newsome, D.J. Anderson, C.I. Bargmann, E.N. Brown, K. Deisseroth, J.P. Donoghue, K.L. Hudson, G.S. Ling, P.R. MacLeish, The BRAIN Initiative: developing technology to catalyse neuroscience discovery, Philosophical Transactions of the Royal Society B: Biological Sciences 370(1668) (2015) 20140164 https://doi.org/10.1098/rstb.2014.0164.
6. C.T. Moritz, Now is the critical time for engineered neuroplasticity, Neurotherapeutics 15(3) (2018) 628-634 https://doi.org/10.1007/s13311-018-0637-0.
7. C.W. Atcherley, N.D. Laude, K.L. Parent, M.L. Heien, Fast-scan controlled-adsorption voltammetry for the quantification of absolute concentrations and adsorption dynamics, Langmuir 29(48) (2013) 14885-14892.
8. E.C. Rutherford, F. Pomerleau, P. Huettl, I. Strömberg, G.A. Gerhardt, Chronic second-by-second measures of l-glutamate in the central nervous system of freely moving rats, Journal of neurochemistry 102(3) (2007) 712-722.
9. D.J. Edell, V.V. Toi, V.M. McNeil, L. Clark, Factors influencing the biocompatibility of insertable silicon microshafts in cerebral cortex, IEEE Transactions on Biomedical Engineering 39(6) (1992) 635-643.
10. D. Szarowski, M. Andersen, S. Retterer, A. Spence, M. Isaacson, H.G. Craighead, J. Turner, W. Shain, Brain responses to micro-machined silicon devices, Brain research 983(1-2) (2003) 23-35.
11. T.D. Kozai, A.S. Jaquins-Gerstl, A.L. Vazquez, A.C. Michael, X.T. Cui, Brain tissue responses to neural implants impact signal sensitivity and intervention strategies, ACS chemical neuroscience 6(1) (2015) 48-67.
12. R.C. Engstrom, R.M. Wightman, E.W. Kristensen, Diffusional distortion in the monitoring of dynamic events, Analytical Chemistry 60(7) (1988) 652-656.
13. K. Kawagoe, P. Garris, D. Wiedemann, R. Wightman, Regulation of transient dopamine concentration gradients in the microenvironment surrounding nerve terminals in the rat striatum, Neuroscience 51(1) (1992) 55-64.
14. H.N. Schwerdt, M. Kim, E. Karasan, S. Amemori, D. Homma, H. Shimazu, T. Yoshida, R. Langer, A.M. Graybiel, M.J. Cima, Subcellular electrode arrays for multisite recording of dopamine in vivo, 2017 IEEE 30th International Conference on Micro Electromechanical Systems (MEMS), IEEE, 2017, pp. 549-552.
15. E. Castagnola, X.S. Zheng, X.T. Cui, Flexible and soft materials and devices for neural interface, Handbook of Neuroengineering, Springer2023, pp. 79-139.
16. L. Luan, J.T. Robinson, B. Aazhang, T. Chi, K. Yang, X. Li, H. Rathore, A. Singer, S. Yellapantula, Y. Fan, Recent advances in electrical neural interface engineering: minimal invasiveness, longevity, and scalability, Neuron 108(2) (2020) 302-321.

17. L. Luan, X. Wei, Z. Zhao, J.J. Siegel, O. Potnis, C.A. Tuppen, S. Lin, S. Kazmi, R.A. Fowler, S. Holloway, Ultraflexible nanoelectronic probes form reliable, glial scar–free neural integration, Science advances 3(2) (2017) e1601966.

18. X. Wei, L. Luan, Z. Zhao, X. Li, H. Zhu, O. Potnis, C. Xie, Nanofabricated ultraflexible electrode arrays for high-density intracortical recording, Advanced Science 5(6) (2018) 1700625.

19. Z. Zhao, H. Zhu, X. Li, L. Sun, F. He, J.E. Chung, D.F. Liu, L. Frank, L. Luan, C. Xie, Ultraflexible electrode arrays for months-long high-density electrophysiological mapping of thousands of neurons in rodents, Nature biomedical engineering 7(4) (2023) 520-532.

20. X. Dai, G. Hong, T. Gao, C.M. Lieber, Mesh nanoelectronics: seamless integration of electronics with tissues, Accounts of chemical research 51(2) (2018) 309-318.

21. J.M. Lee, G. Hong, D. Lin, T.G. Schuhmann Jr, A.T. Sullivan, R.D. Viveros, H.-G. Park, C.M. Lieber, Nanoenabled direct contact interfacing of syringe-injectable mesh electronics, Nano letters 19(8) (2019) 5818-5826.

22. X.S. Zheng, Q. Yang, A. Vazquez, X.T. Cui, Imaging the stability of chronic electrical microstimulation using electrodes coated with PEDOT/CNT and iridium oxide, IScience 25(7) (2022).

23. Y.-M. Chen, T.-W. Chung, P.-W. Wu, P.-C. Chen, A cost-effective fabrication of iridium oxide films as biocompatible electrostimulation electrodes for neural interface applications, Journal of Alloys and Compounds 692 (2017) 339-345.

24. R.D. Meyer, S.F. Cogan, T.H. Nguyen, R.D. Rauh, Electrodeposited iridium oxide for neural stimulation and recording electrodes, IEEE Transactions on Neural Systems and Rehabilitation Engineering 9(1) (2001) 2-11.

25. S. Negi, R. Bhandari, L. Rieth, F. Solzbacher, In vitro comparison of sputtered iridium oxide and platinum-coated neural implantable microelectrode arrays, Biomedical materials 5(1) (2010) 015007.

26. S.F. Cogan, Neural stimulation and recording electrodes, Annu. Rev. Biomed. Eng. 10(1) (2008) 275-309.

27. Q. Yang, B. Wu, E. Castagnola, M.Y. Pwint, N.P. Williams, A.L. Vazquez, X.T. Cui, Integrated Microprism and Microelectrode Array for Simultaneous Electrophysiology and Two-Photon Imaging across All Cortical Layers, Advanced Healthcare Materials (2024) 2302362.

28. C. Boehler, D.M. Vieira, U. Egert, M. Asplund, NanoPt—a nanostructured electrode coating for neural recording and microstimulation, ACS applied materials & interfaces 12(13) (2020) 14855-14865.

29. C. Boehler, F. Oberueber, T. Stieglitz, M. Asplund, Nanostructured platinum as an electrochemically and mechanically stable electrode coating, 2017 39th Annual International Conference of the IEEE Engineering in Medicine and Biology Society (EMBC), IEEE, 2017, pp. 1058-1061.

30. B. Wu, E. Castagnola, C.A. McClung, X.T. Cui, PEDOT/CNT Flexible MEAs Reveal New Insights into the Clock Gene's Role in Dopamine Dynamics, Advanced Science (2024) 2308212.

31. V. Castagnola, C. Bayon, E. Descamps, C. Bergaud, Morphology and

32. X. Cui, V.A. Lee, Y. Raphael, J.A. Wiler, J.F. Hetke, D.J. Anderson, D.C. Martin, Surface modification of neural recording electrodes with conducting polymer/biomolecule blends, Journal of Biomedical Materials Research: An Official Journal of The Society for Biomaterials, The Japanese Society for Biomaterials, and The Australian Society for Biomaterials and the Korean Society for Biomaterials 56(2) (2001) 261-272.

33. X. Cui, D.C. Martin, Electrochemical deposition and characterization of poly (3, 4-ethylenedioxythiophene) on neural microelectrode arrays, Sensors and Actuators B: Chemical 89(1-2) (2003) 92-102.

34. E. Castagnola, L. Maiolo, E. Maggiolini, A. Minotti, M. Marrani, F. Maita, A. Pecora, G.N. Angotzi, A. Ansaldo, L. Fadiga, Ultra-flexible and brain-conformable micro-electrocorticography device with low impedance PEDOT-carbon nanotube coated microelectrodes, 2013 6th International IEEE/EMBS Conference on Neural Engineering (NER), IEEE, 2013, pp. 927-930.

35. E. Castagnola, A. Ansaldo, E. Maggiolini, T. Ius, M. Skrap, D. Ricci, L. Fadiga, Smaller, softer, lower-impedance electrodes for human neuroprosthesis: a pragmatic approach, Frontiers in neuroengineering 7 (2014) 8.

36. D. Khodagholy, J.N. Gelinas, T. Thesen, W. Doyle, O. Devinsky, G.G. Malliaras, G. Buzsáki, NeuroGrid: recording action potentials from the surface of the brain, Nature neuroscience 18(2) (2015) 310-315.

37. M. Asplund, T. Nyberg, O. Inganäs, Electroactive polymers for neural interfaces, Polymer Chemistry 1(9) (2010) 1374-1391.

38. E. Castagnola, E.M. Robbins, B. Wu, M.Y. Pwint, R. Garg, T. Cohen-Karni, X.T. Cui, Flexible glassy carbon multielectrode array for in vivo multisite detection of tonic and phasic dopamine concentrations, Biosensors 12(7) (2022) 540.

39. B. Wu, E. Castagnola, X.T. Cui, Zwitterionic polymer coated and aptamer functionalized flexible micro-electrode arrays for in vivo cocaine sensing and electrophysiology, Micromachines 14(2) (2023) 323.

40. M.L. Huffman, B.J. Venton, Carbon-fiber microelectrodes for in vivo applications, Analyst 134(1) (2009) 18-24.

41. P. Puthongkham, B.J. Venton, Recent advances in fast-scan cyclic voltammetry, Analyst 145(4) (2020) 1087-1102.

42. B.K. Swamy, B.J. Venton, Subsecond detection of physiological adenosine concentrations using fast-scan cyclic voltammetry, Analytical chemistry 79(2) (2007) 744-750.

43. B.J. Venton, Q. Cao, Fundamentals of fast-scan cyclic voltammetry for dopamine detection, Analyst 145(4) (2020) 1158-1168.

44. E. Castagnola, E.M. Robbins, K.M. Woeppel, M. McGuier, A. Golabchi, I.M. Taylor, A.C. Michael, X.T. Cui, Real-time fast scan cyclic voltammetry detection and quantification of exogenously administered melatonin in mice brain, Frontiers in bioengineering and biotechnology 8 (2020) 602216.

45. E. Castagnola, K. Woeppel, A. Golabchi, M. McGuier, N. Chodapaneedi, J. Metro, I.M. Taylor, X.T. Cui, Electrochemical detection of exogenously administered melatonin in the brain, Analyst 145(7) (2020) 2612-2620.

46. A.L. Hensley, A.R. Colley, A.E. Ross, Real-time detection of melatonin using fast-scan cyclic voltammetry, Analytical chemistry 90(14) (2018) 8642-8650.

47. C. Tan, E.M. Robbins, B. Wu, X.T. Cui, Recent advances in in vivo neurochemical monitoring, Micromachines 12(2) (2021) 208.

48. S.J. Updike, M.C. Shults, R.K. Rhodes, B.J. Gilligan, J.O. Luebow, D. Von Heimburg, Enzymatic glucose sensors: improved long-term performance: in vitro: and: in vivo, Asaio Journal 40(2) (1994) 157-163.

49. E.M. Robbins, B. Wong, M.Y. Pwint, S. Salavatian, A. Mahajan, X.T. Cui, Improving Sensitivity and Longevity of In Vivo Glutamate Sensors with Electrodeposited NanoPt, ACS Applied Materials & Interfaces 16(31) (2024) 40570-40580.

50. S. Salavatian, E.M. Robbins, Y. Kuwabara, E. Castagnola, X.T. Cui, A. Mahajan, Real-time in vivo thoracic spinal glutamate sensing during myocardial ischemia, American Journal of Physiology-Heart and Circulatory Physiology 325(6) (2023) H1304-H1317.

51. S. Billa, Y. Yanamadala, I. Hossain, S. Siddiqui, N. Moldovan, T.A. Murray, P.U. Arumugam, Brain-implantable multifunctional probe for simultaneous detection of glutamate and GABA neurotransmitters: optimization and in vivo studies, Micromachines 13(7) (2022) 1008.

52. Z. Hu, Y. Li, G. Figueroa-Miranda, S. Musall, H. Li, M.A. Martínez-Roque, Q. Hu, L. Feng, D. Mayer, A. Offenhäusser, Aptamer based biosensor platforms for neurotransmitters analysis, TrAC Trends in Analytical Chemistry 162 (2023) 117021.

53. G. Wu, N. Zhang, A. Matarasso, I. Heck, H. Li, W. Lu, J.G. Phaup, M.J. Schneider, Y. Wu, Z. Weng, Implantable aptamer-graphene microtransistors for real-time monitoring of neurochemical release in vivo, Nano letters 22(9) (2022) 3668-3677.

54. A.M. Downs, K.W. Plaxco, Real-time, in vivo molecular monitoring using electrochemical aptamer based sensors: opportunities and challenges, ACS sensors 7(10) (2022) 2823-2832.

55. A.A. Grace, Dysregulation of the dopamine system in the pathophysiology of schizophrenia and depression, Nature Reviews Neuroscience 17(8) (2016) 524-532.

56. A.A. Grace, The tonic/phasic model of dopamine system regulation and its implications for understanding alcohol and psychostimulant craving, Addiction 95(8s2) (2000) 119-128.

57. L. Zhang, W.M. Doyon, J.J. Clark, P.E. Phillips, J.A. Dani, Controls of tonic and phasic dopamine transmission in the dorsal and ventral striatum, Molecular pharmacology 76(2) (2009) 396-404.

58. R.A. Saylor, M. Hersey, A. West, A.M. Buchanan, S.N. Berger, H.F. Nijhout, M.C. Reed, J. Best, P. Hashemi, In vivo hippocampal serotonin dynamics in male and female mice: Determining effects of acute escitalopram using fast scan cyclic voltammetry, Frontiers in neuroscience 13 (2019) 362.

59. I. Mitch Taylor, A. Jaquins-Gerstl, S.R. Sesack, A.C. Michael, Domain-dependent effects of DAT inhibition in the rat dorsal striatum, Journal of neurochemistry 122(2) (2012) 283-294.

60. I.M. Taylor, K.M. Nesbitt, S.H. Walters, E.L. Varner, Z. Shu, K.M. Bartlow, A.S. Jaquins-Gerstl, A.C. Michael, Kinetic diversity of dopamine transmission in the dorsal striatum, Journal of neurochemistry 133(4) (2015) 522-531.

61. H. Rafi, A.G. Zestos, Recent advances in FSCV detection of neurochemicals via waveform and carbon microelectrode modification, Journal of The Electrochemical Society 168(5) (2021) 057520.

62. J.G. Roberts, L.A. Sombers, Fast scan cyclic voltammetry: Chemical sensing in the brain and beyond, Analytical chemistry 90(1) (2018) 490.

63. C.J. Meunier, L.A. Sombers, Fast-scan voltammetry for in vivo measurements of neurochemical dynamics, The brain reward system (2021) 93-123.

64. R.B. Keithley, P. Takmakov, E.S. Bucher, A.M. Belle, C.A. Owesson-White, J. Park, R.M. Wightman, Higher sensitivity dopamine measurements with faster-scan cyclic voltammetry, Analytical chemistry 83(9) (2011) 3563-3571.

65. J.G. Roberts, J.V. Toups, E. Eyualem, G.S. McCarty, L.A. Sombers, In situ electrode calibration strategy for voltammetric measurements in vivo, Analytical chemistry 85(23) (2013) 11568-11575.

66. M. Ganesana, S.T. Lee, Y. Wang, B.J. Venton, Analytical techniques in neuroscience: recent advances in imaging, separation, and electrochemical methods, Analytical chemistry 89(1) (2017) 314-341.

67. S. Hafizi, Z.L. Kruk, J.A. Stamford, Fast cyclic voltammetry: improved sensitivity to dopamine with extended oxidation scan limits, Journal of neuroscience methods 33(1) (1990) 41-49.

68. M.L. Heien, P.E. Phillips, G.D. Stuber, A.T. Seipel, R.M. Wightman, Overoxidation of carbon-fiber microelectrodes enhances dopamine adsorption and increases sensitivity, Analyst 128(12) (2003) 1413-1419.

69. B.P. Jackson, S.M. Dietz, R.M. Wightman, Fast-scan cyclic voltammetry of 5-hydroxytryptamine, Analytical chemistry 67(6) (1995) 1115-1120.

70. K.E. Dunham, B.J. Venton, Improving serotonin fast-scan cyclic voltammetry detection: new waveforms to reduce electrode fouling, Analyst 145(22) (2020) 7437-7446.

71. S.E. Cooper, B.J. Venton, Fast-scan cyclic voltammetry for the detection of tyramine and octopamine, Analytical and bioanalytical chemistry 394 (2009) 329-336.

72. J.G. Roberts, L.Z. Lugo-Morales, P.L. Loziuk, L.A. Sombers, Real-time chemical measurements of dopamine release in the brain, Dopamine: methods and protocols (2013) 275-294.

73. P. Cavelier, M. Hamann, D. Rossi, P. Mobbs, D. Attwell, Tonic excitation and inhibition of neurons: ambient transmitter sources and computational consequences, Progress in biophysics and molecular biology 87(1) (2005) 3-16.

74. M. Sarter, C. Lustig, Forebrain cholinergic signaling: wired and phasic, not tonic, and causing behavior, Journal of Neuroscience 40(4) (2020) 712-719.

75. L.M.T.-G. Ruivo, K.L. Baker, M.W. Conway, P.J. Kinsley, G. Gilmour, K.G. Phillips, J.T. Isaac, J.P. Lowry, J.R. Mellor, Coordinated acetylcholine release in prefrontal cortex and hippocampus is associated with arousal and reward on distinct timescales, Cell reports 18(4) (2017) 905-917.

76. A.A. Grace, Phasic versus tonic dopamine release and the modulation of dopamine system responsivity: a hypothesis for the etiology of schizophrenia, Neuroscience 41(1) (1991) 1-24.

77. A.A. Grace, The tonic/phasic model of dopamine system regulation: its relevance for understanding how stimulant abuse can alter basal ganglia function, Drug and alcohol dependence 37(2) (1995) 111-129.

78. E.A. Budygin, C.E. Bass, V.P. Grinevich, A.L. Deal, K.D. Bonin, J.L. Weiner, Opposite consequences of tonic and phasic increases in accumbal dopamine on alcohol-seeking behavior, IScience 23(3) (2020).

79. A. Ledo, C.F. Lourenco, J. Laranjinha, G.A. Gerhardt, R.M. Barbosa, Concurrent measurements of neurochemical and electrophysiological activity with microelectrode arrays: new perspectives for constant potential amperometry, Current Opinion in Electrochemistry 12 (2018) 129-140.

doi:10.20944/preprints202501.0820.v1

25 of 33

80. M.D. Johnson, R.K. Franklin, M.D. Gibson, R.B. Brown, D.R. Kipke, Implantable microelectrode arrays for simultaneous electrophysiological and neurochemical recordings, Journal of Neuroscience Methods 174(1) (2008) 62-70.

81. M. Lundblad, D.A. Price, J.J. Burmeister, J.E. Quintero, P. Huettl, F. Pomerleau, N.R. Zahniser, G.A. Gerhardt, Tonic and phasic amperometric monitoring of dopamine using microelectrode arrays in rat striatum, Applied Sciences 10(18) (2020) 6449.

82. J.E. Quintero, F. Pomerleau, P. Huettl, K.W. Johnson, J. Offord, G.A. Gerhardt, Methodology for rapid measures of glutamate release in rat brain slices using ceramic-based microelectrode arrays: basic characterization and drug pharmacology, Brain research 1401 (2011) 1-9.

83. E. Rand, A. Periyakaruppan, Z. Tanaka, D.A. Zhang, M.P. Marsh, R.J. Andrews, K.H. Lee, B. Chen, M. Meyyappan, J.E. Koehne, A carbon nanofiber-based biosensor for simultaneous detection of dopamine and serotonin in the presence of ascorbicacid, Biosensors and Bioelectronics 42 (2013) 434-438.

84. C. Tan, P.T. Doughty, K. Magee, T.A. Murray, S. Siddiqui, P.U. Arumugam, Effect of process parameters on electrochemical performance of a glutamate microbiosensor, Journal of the Electrochemical Society 167(2) (2020) 027528.

85. J.J. Burmeister, M. Palmer, G.A. Gerhardt, Ceramic-based multisite microelectrode array for rapid choline measures in brain tissue, Analytica chimica acta 481(1) (2003) 65-74.

86. J.J. Burmeister, F. Pomerleau, P. Huettl, C.R. Gash, C.E. Werner, J.P. Bruno, G.A. Gerhardt, Ceramic-based multisite microelectrode arrays for simultaneous measures of choline and acetylcholine in CNS, Biosensors and bioelectronics 23(9) (2008) 1382-1389.

87. C.E. Mattinson, J.J. Burmeister, J.E. Quintero, F. Pomerleau, P. Huettl, G.A. Gerhardt, Tonic and phasic release of glutamate and acetylcholine neurotransmission in sub-regions of the rat prefrontal cortex using enzyme-based microelectrode arrays, Journal of neuroscience methods 202(2) (2011) 199-208.

88. T.T.-C. Tseng, H.G. Monbouquette, Implantable microprobe with arrayed microsensors for combined amperometric monitoring of the neurotransmitters, glutamate and dopamine, Journal of Electroanalytical Chemistry 682 (2012) 141-146.

89. C.W. Atcherley, Voltammetric Measurements Of Tonic And Phasic Neurotransmission, (2014).

90. M.H. Burrell, C.W. Atcherley, M.L. Heien, J. Lipski, A novel electrochemical approach for prolonged measurement of absolute levels of extracellular dopamine in brain slices, ACS chemical neuroscience 6(11) (2015) 1802-1812.

91. A. Abdalla, C.W. Atcherley, P. Pathirathna, S. Samaranayake, B. Qiang, E. Peña, S.L. Morgan, M.L. Heien, P. Hashemi, In vivo ambient serotonin measurements at carbon-fiber microelectrodes, Analytical chemistry 89(18) (2017) 9703-9711.

92. Y. Oh, C. Park, D.H. Kim, H. Shin, Y.M. Kang, M. DeWaele, J. Lee, H.-K. Min, C.D. Blaha, K.E. Bennet, Monitoring in vivo changes in tonic extracellular dopamine level by charge-balancing multiple waveform fast-scan cyclic voltammetry, Analytical chemistry 88(22) (2016) 10962-10970.

93. A.E. Rusheen, T.A. Gee, D.P. Jang, C.D. Blaha, K.E. Bennet, K.H. Lee, M.L. Heien, Y. Oh, Evaluation of electrochemical methods for tonic dopamine detection in vivo, TrAC Trends in Analytical Chemistry 132 (2020) 116049.

94. J.A. Johnson, N.T. Rodeberg, R.M. Wightman, Measurement of basal neurotransmitter levels using convolution-based nonfaradaic current removal, Analytical chemistry 90(12) (2018) 7181-7189.

95. C. Park, Y. Oh, H. Shin, J. Kim, Y. Kang, J. Sim, H.U. Cho, H.K. Lee, S.J. Jung, C.D. Blaha, Fast cyclic square-wave voltammetry to enhance neurotransmitter selectivity and sensitivity, Analytical chemistry 90(22) (2018) 13348-13355.

96. H. Shin, Y. Oh, C. Park, Y. Kang, H.U. Cho, C.D. Blaha, K.E. Bennet, M.L. Heien, I.Y. Kim, K.H. Lee, Sensitive and selective measurement of serotonin in vivo using fast cyclic square-wave voltammetry, Analytical chemistry 92(1) (2019) 774-781.

97. H. Shin, A. Goyal, J.H. Barnett, A.E. Rusheen, J. Yuen, R. Jha, S.M. Hwang, Y. Kang, C. Park, H.-U. Cho, Tonic serotonin measurements in vivo using N-shaped multiple cyclic square wave voltammetry, Analytical chemistry 93(51) (2021) 16987-16994.

98. Y. Oh, M.L. Heien, C. Park, Y.M. Kang, J. Kim, S.L. Boschen, H. Shin, H.U. Cho, C.D. Blaha, K.E. Bennet, Tracking tonic dopamine levels in vivo using multiple cyclic square wave voltammetry, Biosensors and Bioelectronics 121 (2018) 174-182.

99. D.-K. Kim, T.J. Tolliver, S.-J. Huang, B.J. Martin, A.M. Andrews, C. Wichems, A. Holmes, K.-P. Lesch, D.L. Murphy, Altered serotonin synthesis, turnover and dynamic regulation in multiple brain regions of mice lacking the serotonin transporter, Neuropharmacology 49(6) (2005) 798-810.

100. J. Wickens, M. Alexander, R. Miller, Two dynamic modes of striatal function under dopaminergic-cholinergic control: Simulation and analysis of a model, Synapse 8(1) (1991) 1-12.

101. A.G. Salinas, M.I. Davis, D.M. Lovinger, Y. Mateo, Dopamine dynamics and cocaine sensitivity differ between striosome and matrix compartments of the striatum, Neuropharmacology 108 (2016) 275-283.

102. S. Threlfell, S.J. Cragg, Dopamine signaling in dorsal versus ventral striatum: the dynamic role of cholinergic interneurons, Frontiers in systems neuroscience 5 (2011) 11.

103. A.L. Collins, B.T. Saunders, Heterogeneity in striatal dopamine circuits: Form and function in dynamic reward seeking, Journal of neuroscience research 98(6) (2020) 1046-1069.

104. E. Castagnola, Q. Cao, E. Robbins, B. Wu, M.Y. Pwint, U. Siwakoti, X.T. Cui, Glassy Carbon Fiber-Like Multielectrode Arrays for Neurochemical Sensing and Electrophysiology Recording, Advanced Materials Technologies (2024) 2400863.

105. E. Castagnola, E.M. Robbins, D.D. Krahe, B. Wu, M.Y. Pwint, Q. Cao, X.T. Cui, Stable in-vivo electrochemical sensing of tonic serotonin levels using PEDOT/CNT-coated glassy carbon flexible microelectrode arrays, Biosensors and Bioelectronics 230 (2023) 115242.

106. A.S. Pranti, A. Schander, A. Bödecker, W. Lang, PEDOT: PSS coating on gold microelectrodes with excellent stability and high charge injection capacity for chronic neural interfaces, Sensors and Actuators B: Chemical 275 (2018) 382-393.

107. E. Castagnola, S. Carli, M. Vomero, A. Scarpellini, M. Prato, N. Goshi, L. Fadiga, S. Kassegne, D. Ricci, Multilayer poly (3, 4-ethylenedioxythiophene)-dexamethasone and poly (3, 4-ethylenedioxythiophene)-polystyrene sulfonate-carbon nanotubes coatings on glassy carbon microelectrode arrays for controlled drug release, Biointerphases 12(3) (2017).

108. E. Castagnola, L. Maiolo, E. Maggiolini, A. Minotti, M. Marrani, F. Maita, A. Pecora, G.N. Angotzi, A. Ansaldo, M. Boffini, PEDOT-CNT-coated low-impedance, ultra-flexible, and brain-conformable micro-ECoG arrays, IEEE Transactions on Neural Systems and Rehabilitation Engineering 23(3) (2014) 342-350.

109. E. Castagnola, A. Ansaldo, E. Maggiolini, G.N. Angotzi, M. Skrap, D. Ricci, L. Fadiga, Biologically compatible neural interface to safely couple nanocoated electrodes to the surface of the brain, ACS nano 7(5) (2013) 3887-3895.

110. A. Ansaldo, E. Castagnola, E. Maggiolini, L. Fadiga, D. Ricci, Superior electrochemical performance of carbon nanotubes directly grown on sharp microelectrodes, ACS nano 5(3) (2011) 2206-2214.

111. G. Baranauskas, E. Maggiolini, E. Castagnola, A. Ansaldo, A. Mazzoni, G.N. Angotzi, A. Vato, D. Ricci, S. Panzeri, L. Fadiga, Carbon nanotube composite coating of neural microelectrodes preferentially improves the multiunit signal-to-noise ratio, Journal of neural engineering 8(6) (2011) 066013.

112. X. Cui, D.C. Martin, Fuzzy gold electrodes for lowering impedance and improving adhesion with electrodeposited conducting polymer films, Sensors and Actuators A: Physical 103(3) (2003) 384-394.

113. X. Cui, J. Wiler, M. Dzaman, R.A. Altschuler, D.C. Martin, In vivo studies of polypyrrole/peptide coated neural probes, Biomaterials 24(5) (2003) 777-787.

114. H. Shi, C. Liu, Q. Jiang, J. Xu, Effective approaches to improve the electrical conductivity of PEDOT: PSS: a review, Advanced Electronic Materials 1(4) (2015) 1500017.

115. K.M. Woeppel, X.S. Zheng, Z.M. Schulte, N.L. Rosi, X.T. Cui, Nanoparticle doped PEDOT for enhanced electrode coatings and drug delivery, Advanced healthcare materials 8(21) (2019) 1900622.

116. C. Boehler, C. Kleber, N. Martini, Y. Xie, I. Dryg, T. Stieglitz, U. Hofmann, M. Asplund, Actively controlled release of Dexamethasone from neural microelectrodes in a chronic in vivo study, Biomaterials 129 (2017) 176-187.

117. M. Vázquez, J. Bobacka, A. Ivaska, A. Lewenstam, Influence of oxygen and carbon dioxide on the electrochemical stability of poly (3, 4-ethylenedioxythiophene) used as ion-to-electron transducer in all-solid-state ion-selective electrodes, Sensors and Actuators B: Chemical 82(1) (2002) 7-13.

118. V. Castagnola, E. Descamps, A. Lecestre, L. Dahan, J. Remaud, L.G. Nowak, C. Bergaud, Parylene-based flexible neural probes with PEDOT coated surface for brain stimulation and recording, Biosensors and Bioelectronics 67 (2015) 450-457.

119. X.T. Cui, D.D. Zhou, Poly (3, 4-ethylenedioxythiophene) for chronic neural stimulation, IEEE Transactions on Neural Systems and Rehabilitation Engineering 15(4) (2007) 502-508.

120. E. Musk, An integrated brain-machine interface platform with thousands of channels, Journal of medical Internet research 21(10) (2019) e16194.

121. H. Vara, J.E. Collazos-Castro, Enhanced spinal cord microstimulation using conducting polymer-coated carbon microfibers, Acta biomaterialia 90 (2019) 71-86.

122. X.S. Zheng, C. Tan, E. Castagnola, X.T. Cui, Electrode materials for chronic electrical microstimulation, Advanced healthcare materials 10(12) (2021) 2100119.

123. R.A. Green, R.T. Hassarati, L. Bouchinet, C.S. Lee, G.L. Cheong, F.Y. Jin, C.W. Dodds, G.J. Suaning, L.A. Poole-Warren, N.H. Lovell, Substrate dependent stability of conducting polymer coatings on medical electrodes, Biomaterials 33(25) (2012) 5875-5886.

124. L. Ouyang, B. Wei, C.-c. Kuo, S. Pathak, B. Farrell, D.C. Martin, Enhanced PEDOT adhesion on solid substrates with electrografted P (EDOT-NH2), Science advances 3(3) (2017) e1600448.

125. S. Carli, L. Lambertini, E. Zucchini, F. Ciarpella, A. Scarpellini, M. Prato, E. Castagnola, L. Fadiga, D. Ricci, Single walled carbon nanohorns composite for neural sensing and stimulation, Sensors and Actuators B: Chemical 271 (2018) 280-288.

126. X. Luo, C.L. Weaver, D.D. Zhou, R. Greenberg, X.T. Cui, Highly stable carbon nanotube doped poly (3, 4-ethylenedioxythiophene) for chronic neural stimulation, Biomaterials 32(24) (2011) 5551-5557.

127. N.A. Alba, Z.J. Du, K.A. Catt, T.D. Kozai, X.T. Cui, In vivo electrochemical analysis of a PEDOT/MWCNT neural electrode coating, Biosensors 5(4) (2015) 618-646.

128. H. Charkhkar, G.L. Knaack, D.G. McHail, H.S. Mandal, N. Peixoto, J.F. Rubinson, T.C. Dumas, J.J. Pancrazio, Chronic intracortical neural recordings using microelectrode arrays coated with PEDOT–TFB, Acta Biomaterialia 32 (2016) 57-67.

129. I.M. Taylor, N.A. Patel, N.C. Freedman, E. Castagnola, X.T. Cui, Direct in vivo electrochemical detection of resting dopamine using poly (3, 4-ethylenedioxythiophene)/carbon nanotube functionalized microelectrodes, Analytical chemistry 91(20) (2019) 12917-12927.

130. I.M. Taylor, E.M. Robbins, K.A. Catt, P.A. Cody, C.L. Happe, X.T. Cui, Enhanced dopamine detection sensitivity by PEDOT/graphene oxide coating on in vivo carbon fiber electrodes, Biosensors and Bioelectronics 89 (2017) 400-410.

131. R.F. Vreeland, C.W. Atcherley, W.S. Russell, J.Y. Xie, D. Lu, N.D. Laude, F. Porreca, M.L. Heien, Biocompatible PEDOT: Nafion composite electrode coatings for selective detection of neurotransmitters in vivo, Analytical chemistry 87(5) (2015) 2600-2607.

132. W. Cho, F. Liu, A. Hendrix, T. Asrat, V. Connaughton, A.G. Zestos, Timed electrodeposition of PEDOT: Nafion onto carbon fiber-microelectrodes enhances dopamine detection in zebrafish retina, Journal of The Electrochemical Society 167(11) (2020) 115501.

133. S. Demuru, H. Deligianni, Surface PEDOT: nafion coatings for enhanced dopamine, serotonin and adenosine sensing, Journal of The Electrochemical Society 164(14) (2017) G129.

134. T.D. Kozai, K. Catt, Z. Du, K. Na, O. Srivannavit, M.H. Razi-ul, J. Seymour, K.D. Wise, E. Yoon, X.T. Cui, Chronic in vivo evaluation of PEDOT/CNT for stable neural recordings, IEEE transactions on biomedical engineering 63(1) (2015) 111-119.

135. M. Vomero, E. Castagnola, F. Ciarpella, E. Maggiolini, N. Goshi, E. Zucchini, S. Carli, L. Fadiga, S. Kassegne, D. Ricci, Highly stable glassy carbon interfaces for long-term neural stimulation and low-noise recording of brain activity, Scientific reports 7(1) (2017) 40332.

136. S. Nimbalkar, E. Castagnola, A. Balasubramani, A. Scarpellini, S. Samejima, A. Khorasani, A. Boissenin, S. Thongpang, C. Moritz, S. Kassegne, Ultra-capacitive carbon neural probe allows simultaneous long-term electrical stimulations and high-resolution neurotransmitter detection, Scientific reports 8(1) (2018) 6958.

137. R.L. McCreery, Advanced carbon electrode materials for molecular electrochemistry, Chemical reviews 108(7) (2008) 2646-2687.

138. B.L. Hanssen, S. Siraj, D.K. Wong, Recent strategies to minimise fouling in electrochemical detection systems, Reviews in Analytical Chemistry 35(1) (2016) 1-28.

139. E. He, S. Xu, Y. Dai, Y. Wang, G. Xiao, J. Xie, S. Xu, P. Fan, F. Mo, M. Wang, SWCNTs/PEDOT: PSS-modified microelectrode arrays for dual-mode detection of electrophysiological signals and dopamine concentration in the striatum under isoflurane anesthesia, ACS sensors 6(9) (2021) 3377-3386.

140. G. Xiao, S. Xu, Y. Song, Y. Zhang, Z. Li, F. Gao, J. Xie, L. Sha, Q. Xu, Y. Shen, In situ detection of neurotransmitters and epileptiform electrophysiology activity in awake mice brains using a nanocomposites modified microelectrode array, Sensors and Actuators B: Chemical 288 (2019) 601-610.

141. P. Fan, Y. Wang, Y. Dai, L. Jing, W. Liang, B. Lu, G. Yang, Y. Song, Y. Wu, X. Cai, Flexible microelectrode array probe for simultaneous detection of neural discharge and dopamine in striatum of mice aversion system, Sensors and Actuators B: Chemical 390 (2023) 133990.

142. X. Wang, M. Xu, H. Yang, W. Jiang, J. Jiang, D. Zou, Z. Zhu, C. Tao, S. Ni, Z. Zhou, Ultraflexible Neural Electrodes Enabled Synchronized Long-Term Dopamine Detection and Wideband Chronic Recording Deep in Brain, ACS nano (2024).

143. J.J. Burmeister, G.A. Gerhardt, Self-referencing ceramic-based multisite microelectrodes for the detection and elimination of interferences from the measurement of L-glutamate and other analytes, Analytical chemistry 73(5) (2001) 1037-1042.

144. J.J. Burmeister, D.A. Price, F. Pomerleau, P. Huettl, J.E. Quintero, G.A. Gerhardt, Challenges of simultaneous measurements of brain extracellular GABA and glutamate in vivo using enzyme-coated microelectrode arrays, Journal of neuroscience methods 329 (2020) 108435.

145. M. Clay, H.G. Monbouquette, Simulated Performance of Electroenzymatic Glutamate Biosensors In Vivo Illuminates the Complex Connection to Calibration In Vitro, ACS Chemical Neuroscience 12(22) (2021) 4275-4285.

146. S. Qin, M. Van der Zeyden, W.H. Oldenziel, T.I. Cremers, B.H. Westerink, Microsensors for in vivo measurement of glutamate in brain tissue, Sensors 8(11) (2008) 6860-6884.

147. A.A. Disney, C. McKinney, L. Grissom, X. Lu, J.H. Reynolds, A multi-site array for combined local electrochemistry and electrophysiology in the non-human primate brain, Journal of neuroscience methods 255 (2015) 29-37.

148. X. Liu, J. Liu, Biosensors and sensors for dopamine detection, View 2(1) (2021) 20200102.

149. S. Baluta, D. Zając, A. Szyszka, K. Malecha, J. Cabaj, Enzymatic platforms for sensitive neurotransmitter detection, Sensors 20(2) (2020) 423.

150. J.L. Scoggin, C. Tan, N.H. Nguyen, U. Kansakar, M. Madadi, S. Siddiqui, P.U. Arumugam, M.A. DeCoster, T.A. Murray, An enzyme-based electrochemical biosensor probe with sensitivity to detect astrocytic versus glioma uptake of glutamate in real time in vitro, Biosensors and Bioelectronics 126 (2019) 751-757.

151. U. Chae, J. Woo, Y. Cho, J.-K. Han, S.H. Yang, E. Yang, H. Shin, H. Kim, H.-Y. Yu, C.J. Lee, A neural probe for concurrent real-time measurement of multiple neurochemicals with electrophysiology in multiple brain regions in vivo, Proceedings of the National Academy of Sciences 120(28) (2023) e2219231120.

152. G. Xiao, Y. Song, S. Zhang, L. Yang, S. Xu, Y. Zhang, H. Xu, F. Gao, Z. Li, X. Cai, A high-sensitive nano-modified biosensor for dynamic monitoring of glutamate and neural spike covariation from rat cortex to hippocampal sub-regions, Journal of Neuroscience Methods 291 (2017) 122-130.

153. W. Wei, Y. Song, L. Wang, S. Zhang, J. Luo, S. Xu, X. Cai, An implantable microelectrode array for simultaneous L-glutamate and electrophysiological recordings in vivo, Microsystems & Nanoengineering 1(1) (2015) 1-6.

154. C. Ziegler, W. Göpel, Biosensor development, Current opinion in chemical biology 2(5) (1998) 585-591.

155. G. Rocchitta, A. Spanu, S. Babudieri, G. Latte, G. Madeddu, G. Galleri, S. Nuvoli, P. Bagella, M.I. Demartis, V. Fiore, Enzyme biosensors for biomedical applications: Strategies for safeguarding analytical performances in biological fluids, Sensors 16(6) (2016) 780.

156. J.I. Reyes-De-Corcuera, H.E. Olstad, R. García-Torres, Stability and stabilization of enzyme biosensors: the key to successful application and commercialization, Annual review of food science and technology 9(1) (2018) 293-322.

157. Y. Li, Y. Bai, G. Han, M. Li, Porous-reduced graphene oxide for fabricating an amperometric acetylcholinesterase biosensor, Sensors and actuators B: Chemical 185 (2013) 706-712.

158. G. Sun, X. Wei, D. Zhang, L. Huang, H. Liu, H. Fang, Immobilization of enzyme electrochemical biosensors and their application to food bioprocess monitoring, Biosensors 13(9) (2023) 886.

159. O. Prakash, D. Verma, P.C. Singh, Exploring the Potential of Enzyme-Immobilized MOFs: Biosensing, Biocatalysis, Targeted Drug Delivery and Cancer Therapy, Journal of Materials Chemistry B (2024).

160. J. Jang, H.-U. Cho, S. Hwang, Y. Kwak, H. Kwon, M.L. Heien, K.E. Bennet, Y. Oh, H. Shin, K.H. Lee, Understanding the different effects of fouling mechanisms on working and reference electrodes in fast-scan cyclic voltammetry for neurotransmitter detection, Analyst 149(10) (2024) 3008-3016.

161. S. Campuzano, M. Pedrero, P. Yáñez-Sedeño, J.M. Pingarrón, Antifouling (bio) materials for electrochemical (bio) sensing, International journal of molecular sciences 20(2) (2019) 423.

162. G.S. Wilson, R. Gifford, Biosensors for real-time in vivo measurements, Biosensors and Bioelectronics 20(12) (2005) 2388-2403.

163. B.R. Baker, R.Y. Lai, M.S. Wood, E.H. Doctor, A.J. Heeger, K.W. Plaxco, An electronic, aptamer-based small-molecule sensor for the rapid, label-free detection of cocaine in adulterated samples and biological fluids, Journal of the American Chemical Society 128(10) (2006) 3138-3139.

164. C. Zhao, K.M. Cheung, I.-W. Huang, H. Yang, N. Nakatsuka, W. Liu, Y. Cao, T. Man, P.S. Weiss, H.G. Monbouquette, Implantable aptamer–field-effect transistor neuroprobes for in vivo neurotransmitter monitoring, Science advances 7(48) (2021) eabj7422.

165. H. Chen, M. Xiao, J. He, Y. Zhang, Y. Liang, H. Liu, Z. Zhang, Aptamer-functionalized carbon nanotube field-effect transistor biosensors for Alzheimer's disease serum biomarker detection, ACS sensors 7(7) (2022) 2075-2083.

166. W. Fu, L. Jiang, E.P. van Geest, L.M. Lima, G.F. Schneider, Sensing at the surface of graphene field-effect transistors, Advanced Materials 29(6) (2017) 1603610.

167. D. Sadighbayan, M. Hasanzadeh, E. Ghafar-Zadeh, Biosensing based on field-effect transistors (FET): Recent progress and challenges, TrAC Trends in Analytical Chemistry 133 (2020) 116067.

168. N.S. Green, M.L. Norton, Interactions of DNA with graphene and sensing applications of graphene field-effect transistor devices: A review, Analytica chimica acta 853 (2015) 127-142.

169. R. Ziółkowski, M. Jarczewska, Ł. Górski, E. Malinowska, From small molecules toward whole cells detection: Application of electrochemical aptasensors in modern medical diagnostics, Sensors 21(3) (2021) 724.

170. F.V. Oberhaus, D. Frense, D. Beckmann, Immobilization techniques for aptamers on gold electrodes for the electrochemical detection of proteins: a review, Biosensors 10(5) (2020) 45.

171. I. Grabowska, M. Hepel, K. Kurzątkowska-Adaszyńska, Advances in design strategies of multiplex electrochemical aptasensors, Sensors 22(1) (2021) 161.

172. D. Kang, R.J. White, F. Xia, X. Zuo, A. Vallée-Bélisle, K.W. Plaxco, DNA biomolecular-electronic encoder and decoder devices constructed by multiplex biosensors, NPG Asia Materials 4(1) (2012) e1-e1.

173. I.M. Taylor, Z. Du, E.T. Bigelow, J.R. Eles, A.R. Horner, K.A. Catt, S.G. Weber, B.G. Jamieson, X.T. Cui, Aptamer-functionalized neural recording electrodes for the direct measurement of cocaine in vivo, Journal of Materials Chemistry B 5(13) (2017) 2445-2458.

174. Y. Wen, H. Pei, Y. Wan, Y. Su, Q. Huang, S. Song, C. Fan, DNA nanostructure-decorated surfaces for enhanced aptamer-target binding and electrochemical cocaine sensors, Analytical chemistry 83(19) (2011) 7418-7423.

175. Y. Liu, L. Kong, H. Li, R. Yuan, Y. Chai, Electrochemical aptamer biosensor based on ATP-induced 2D DNA structure switching for rapid and ultrasensitive detection of ATP, Analytical Chemistry 94(18) (2022) 6819-6826.

176. Y. Jiang, W. Ma, W. Ji, H. Wei, L. Mao, Aptamer superstructure-based electrochemical biosensor for sensitive detection of ATP in rat brain with in vivo microdialysis, Analyst 144(5) (2019) 1711-1717.

177. A. Hellmann, A. Schundner, M. Frick, C. Kranz, Electrochemical detection of ATP release in-vitro and in-vivo, Current Opinion in Electrochemistry 39 (2023) 101282.

178. A. Azadbakht, M. Roushani, A.R. Abbasi, Z. Derikvand, Design and characterization of electrochemical dopamine–aptamer as convenient and integrated sensing platform, Analytical biochemistry 507 (2016) 47-57.

179. H. Abu-Ali, C. Ozkaya, F. Davis, N. Walch, A. Nabok, Electrochemical aptasensor for detection of dopamine, Chemosensors 8(2) (2020) 28.

180. S.N. Cuhadar, H. Durmaz, N. Yildirim-Tirgil, Multi-detection of seratonin and dopamine based on an electrochemical aptasensor, Chemical Papers 78(12) (2024) 7175-7185.

181. J. Li, Y. Si, Y.E. Park, J.-S. Choi, S.M. Jung, J.E. Lee, H.J. Lee, A serotonin voltammetric biosensor composed of carbon nanocomposites and DNA aptamer, Microchimica Acta 188 (2021) 1-8.

182. R. Li, X. Li, L. Su, H. Qi, X. Yue, H. Qi, Label-free Electrochemical Aptasensor for the Determination of Serotonin, Electroanalysis 34(6) (2022) 1048-1053.

183. A. Golabchi, B. Wu, B. Cao, C.J. Bettinger, X.T. Cui, Zwitterionic polymer/polydopamine coating reduce acute inflammatory tissue responses to neural implants, Biomaterials 225 (2019) 119519.

184. Q. Yang, B. Wu, J.R. Eles, A.L. Vazquez, T.D. Kozai, X.T. Cui, Zwitterionic polymer coating suppresses microglial encapsulation to neural implants in vitro and in vivo, Advanced biosystems 4(6) (2020) 1900287.

185. P. Puthongkham, B.J. Venton, Recent Advances in Fast-Scan Cyclic Voltammetry, Analyst 145 (2020) 1087-1102 DOI: 10.1039/C9AN01925A.

186. C. Yang, M.E. Denno, P. Pyakurel, B.J. Venton, Recent trends in carbon nanomaterial-based electrochemical sensors for biomolecules: A review, Analytica chimica acta 887 (2015) 17-37.

187. E. Castagnola, R. Garg, S.K. Rastogi, T. Cohen-Karni, X.T. Cui, 3D fuzzy graphene microelectrode array for dopamine sensing at sub-cellular spatial resolution, Biosensors and Bioelectronics 191 (2021) 113440.

188. M. Devi, M. Vomero, E. Fuhrer, E. Castagnola, C. Gueli, S. Nimbalkar, M. Hirabayashi, S. Kassegne, T. Stieglitz, S. Sharma, Carbon-based neural electrodes: Promises and challenges, Journal of Neural Engineering 18(4) (2021) 041007.

189. E. Castagnola, A. Ansaldo, L. Fadiga, D. Ricci, Chemical vapour deposited carbon nanotube coated microelectrodes for intracortical neural recording, physica status solidi (b) 247(11-12) (2010) 2703-2707.

190. E.M. Robbins, E. Castagnola, X.T. Cui, Accurate and stable chronic in vivo voltammetry enabled by a replaceable subcutaneous reference electrode, Iscience 25(8) (2022).

191. N.T. Rodeberg, S.G. Sandberg, J.A. Johnson, P.E. Phillips, R.M. Wightman, Hitchhiker's guide to voltammetry: acute and chronic electrodes for in vivo fast-scan cyclic voltammetry, ACS chemical neuroscience 8(2) (2017) 221-234.

192. C.J. Meunier, J.D. Denison, G.S. McCarty, L.A. Sombers, Interpreting dynamic interfacial changes at carbon fiber microelectrodes using electrochemical impedance spectroscopy, Langmuir 36(15) (2020) 4214-4223.

193. T.D.Y. Kozai, N.B. Langhals, P.R. Patel, X. Deng, H. Zhang, K.L. Smith, J. Lahann, N.A. Kotov, D.R. Kipke, Ultrasmall implantable composite microelectrodes with bioactive surfaces for chronic neural interfaces, Nature materials 11(12) (2012) 1065-1073.

194. H.N. Schwerdt, E. Zhang, M.J. Kim, T. Yoshida, L. Stanwicks, S. Amemori, H.E. Dagdeviren, R. Langer, M.J. Cima, A.M. Graybiel, Cellular-scale probes enable stable chronic subsecond monitoring of dopamine neurochemicals in a rodent model, Communications biology 1(1) (2018) 144.

195. G. Guitchounts, D. Cox, 64-channel carbon fiber electrode arrays for chronic electrophysiology, Scientific Reports 10(1) (2020) 3830.

196. P.R. Patel, P. Popov, C.M. Caldwell, E.J. Welle, D. Egert, J.R. Pettibone, D.H. Roossien, J.B. Becker, J.D. Berke, C.A. Chestek, High density carbon fiber arrays for chronic electrophysiology, fast scan cyclic voltammetry, and correlative anatomy, Journal of Neural Engineering 17(5) (2020) 056029.

197. H.N. Schwerdt, D.J. Gibson, K. Amemori, L.L. Stanwicks, T. Yoshida, M.J. Cima, A.M. Graybiel, Chronic multi-modal monitoring of neural activity in rodents and primates, Integrated Sensors for Biological and Neural Sensing, SPIE, 2021, pp. 11-17.

198. H. Schwerdt, K. Amemori, D. Gibson, L. Stanwicks, T. Yoshida, N. Bichot, S. Amemori, R. Desimone, R. Langer, M. Cima, Dopamine and beta-band oscillations differentially link to striatal value and motor control, Science Advances 6(39) (2020) eabb9226.

199. E.J. Welle, P.R. Patel, J.E. Woods, A. Petrossians, E. Della Valle, A. Vega-Medina, J.M. Richie, D. Cai, J.D. Weiland, C.A. Chestek, Ultra-small carbon fiber electrode recording site optimization and improved in vivo chronic recording yield, Journal of neural engineering 17(2) (2020) 026037.

200. P.R. Patel, K. Na, H. Zhang, T.D. Kozai, N.A. Kotov, E. Yoon, C.A. Chestek, Insertion of linear 8.4 μm diameter 16 channel carbon fiber electrode arrays for single unit recordings, Journal of neural engineering 12(4) (2015) 046009.

201. H.N. Schwerdt, M.J. Kim, S. Amemori, D. Homma, T. Yoshida, H. Shimazu, H. Yerramreddy, E. Karasan, R. Langer, A.M. Graybiel, Subcellular probes for neurochemical recording from multiple brain sites, Lab on a Chip 17(6) (2017) 1104-1115.

202. H.N. Schwerdt, H. Shimazu, K.-i. Amemori, S. Amemori, P.L. Tierney, D.J. Gibson, S. Hong, T. Yoshida, R. Langer, M.J. Cima, Long-term dopamine neurochemical monitoring in primates, Proceedings of the National Academy of Sciences 114(50) (2017) 13260-13265.

203. P.R. Patel, H. Zhang, M.T. Robbins, J.B. Nofar, S.P. Marshall, M.J. Kobylarek, T.D. Kozai, N.A. Kotov, C.A. Chestek, Chronic in vivo stability assessment of carbon fiber microelectrode arrays, Journal of neural engineering 13(6) (2016) 066002.

204. B. Fan, C.A. Rusinek, C.H. Thompson, M. Setien, Y. Guo, R. Rechenberg, Y. Gong, A.J. Weber, M.F. Becker, E. Purcell, Flexible, diamond-based microelectrodes fabricated using the diamond growth side for neural sensing, Microsystems & nanoengineering 6(1) (2020) 42.

205. M. Vomero, P. Van Niekerk, V. Nguyen, N. Gong, M. Hirabayashi, A. Cinopri, K. Logan, A. Moghadasi, P. Varma, S. Kassegne, A novel pattern transfer technique for mounting glassy carbon microelectrodes on polymeric flexible substrates, Journal of Micromechanics and Microengineering 26(2) (2016) 025018.

206. E. Castagnola, S. Thongpang, M. Hirabayashi, G. Nava, S. Nimbalkar, T. Nguyen, S. Lara, A. Oyawale, J. Bunnell, C. Moritz, Glassy carbon microelectrode arrays enable voltage-peak separated simultaneous detection of dopamine and serotonin using fast scan cyclic voltammetry, Analyst 146(12) (2021) 3955-3970.

207. S. Kassegne, M. Vomero, R. Gavuglio, M. Hirabayashi, E. Özyilmaz, S. Nguyen, J. Rodriguez, E. Özyilmaz, P. van Niekerk, A. Khosla, Electrical impedance, electrochemistry, mechanical stiffness, and hardness tunability in glassy carbon MEMS μECoG electrodes, Microelectronic Engineering 133 (2015) 36-44.

208. N.W. Vahidi, S. Rudraraju, E. Castagnola, C. Cea, S. Nimbalkar, R. Hanna, R. Arvizu, S.A. Dayeh, T.Q. Gentner, S. Kassegne, Epi-Intra neural probes with glassy carbon microelectrodes help elucidate neural coding and stimulus encoding in 3D volume of tissue, Journal of Neural Engineering 17(4) (2020) 046005.

209. N. Goshi, E. Castagnola, M. Vomero, C. Gueli, C. Cea, E. Zucchini, D. Bjanes, E. Maggiolini, C. Moritz, S. Kassegne, Glassy carbon MEMS for novel origami-styled 3D integrated intracortical and epicortical neural probes, Journal of Micromechanics and Microengineering 28(6) (2018) 065009.

210. E. Castagnola, N.W. Vahidi, S. Nimbalkar, S. Rudraraju, M. Thielk, E. Zucchini, C. Cea, S. Carli, T.Q. Gentner, D. Ricci, In vivo dopamine detection and single unit recordings using intracortical glassy carbon microelectrode arrays, MRS advances 3(29) (2018) 1629-1634.

211. E.-B.A. Faul, A.M. Broussard, D.R. Rivera, M.Y. Pwint, B. Wu, Q. Cao, D. Bailey, X.T. Cui, E. Castagnola, Batch Fabrication of Microelectrode Arrays with Glassy Carbon Microelectrodes and Interconnections for Neurochemical Sensing: Promises and Challenges, Micromachines 15(2) (2024) 277.

212. K.-H. Nam, M. Abdulhafez, E. Castagnola, G.N. Tomaraei, X.T. Cui, M. Bedewy, Laser direct write of heteroatom-doped graphene on molecularly controlled polyimides for electrochemical biosensors with nanomolar sensitivity, Carbon 188 (2022) 209-219.

213. R. Ye, D.K. James, J.M. Tour, Laser-induced graphene, Accounts of chemical research 51(7) (2018) 1609-1620.

214. M.G. Stanford, C. Zhang, J.D. Fowlkes, A. Hoffman, I.N. Ivanov, P.D. Rack, J.M. Tour, High-resolution laser-induced graphene. Flexible electronics beyond the visible limit, ACS applied materials & interfaces 12(9) (2020) 10902-10907.

215. J. Lin, Z. Peng, Y. Liu, F. Ruiz-Zepeda, R. Ye, E.L. Samuel, M.J. Yacaman, B.I. Yakobson, J.M. Tour, Laser-induced porous graphene films from commercial polymers, Nature Communications 5(1) (2014) 5714.

216. T.S.D. Le, H.P. Phan, S. Kwon, S. Park, Y. Jung, J. Min, B.J. Chun, H. Yoon, S.H. Ko, S.W. Kim, Recent advances in laser-induced graphene: mechanism, fabrication, properties, and applications in flexible electronics, Advanced Functional Materials 32(48) (2022) 2205158.

217. M. Abdulhafez, G.N. Tomaraei, M. Bedewy, Fluence-dependent morphological transitions in laser-induced graphene electrodes on polyimide substrates for flexible devices, ACS Applied Nano Materials 4(3) (2021) 2973-2986.

218. J. Li, Y. Liu, L. Yuan, B. Zhang, E.S. Bishop, K. Wang, J. Tang, Y.-Q. Zheng, W. Xu, S. Niu, A tissue-like neurotransmitter sensor for the brain and gut, Nature 606(7912) (2022) 94-101.

219. Y. Lee, M.J. Low, D. Yang, H.K. Nam, T.-S.D. Le, S.E. Lee, H. Han, S. Kim, Q.H. Vu, H. Yoo, Ultra-thin light-weight laser-induced-graphene (LIG) diffractive optics, Light: Science & Applications 12(1) (2023) 146.

220. M. Johnson, R. Franklin, K. Scott, R. Brown, D. Kipke, Neural probes for concurrent detection of neurochemical and electrophysiological signals in vivo, 2005 IEEE Engineering in Medicine and Biology 27th Annual Conference, IEEE, 2006, pp. 7325-7328.

221. S. Zhang, Y. Song, M. Wang, Z. Zhang, X. Fan, X. Song, P. Zhuang, F. Yue, P. Chan, X. Cai, A silicon based implantable microelectrode array for electrophysiological and dopamine recording from cortex to striatum in the non-human primate brain, Biosensors and Bioelectronics 85 (2016) 53-61.

222. J.A. Stamford, P. Palij, C. Davidson, C.M. Jorm, J. Millar, Simultaneous "real-time" electrochemical and electrophysiological recording in brain slices with a single carbon-fibre microelectrode, Journal of neuroscience methods 50(3) (1993) 279-290

223. J.F. Cheer, M.L. Heien, P.A. Garris, R.M. Carelli, R.M. Wightman, Simultaneous dopamine and single-unit recordings reveal accumbens GABAergic responses: implications for intracranial self-stimulation, Proceedings of the National Academy of Sciences 102(52) (2005) 19150-19155.

224. L.R. Walton, N.G. Boustead, S. Carroll, R.M. Wightman, Effects of glutamate receptor activation on local oxygen changes, ACS Chemical Neuroscience 8(7) (2017) 1598-1608.

225. C.N. Hobbs, J.A. Johnson, M.D. Verber, R.M. Wightman, An implantable multimodal sensor for oxygen, neurotransmitters, and electrophysiology during spreading depolarization in the deep brain, Analyst 142(16) (2017) 2912-2920.

226. Y. Oh, C. Park, D.H. Kim, H. Shin, Y.M. Kang, M. DeWaele, J. Lee, H.-K. Min, C.D. Blaha, K.E. Bennet, Monitoring in vivo changes in tonic extracellular dopamine level by charge-balancing multiple waveform fast-scan cyclic voltammetry, Analytical chemistry 88(22) (2016) 10962-10970 https://doi.org/10.1021/acs.analchem.6b02605.

227. D.L. Robinson, B.J. Venton, M.L. Heien, R.M. Wightman, Detecting subsecond dopamine release with fast-scan cyclic voltammetry in vivo, Clinical chemistry 49(10) (2003) 1763-1773 https://doi.org/10.1373/49.10.1763.

228. K.M.W.a.P. Hashemi, Fast-Scan Cyclic Voltammetry Analysis of Dynamic Serotonin Reponses to Acute Escitalopram, ACS Chem Neurosci. 4(5) (2013) 715–720 https://doi.org/10.1021/cn4000378.

229. B.K. Swamy, B.J. Venton, Carbon nanotube-modified microelectrodes for simultaneous detection of dopamine and serotonin in vivo, Analyst 132(9) (2007) 876-884.

230. Y. Ou, A.M. Buchanan, C.E. Witt, P. Hashemi, Frontiers in electrochemical sensors for neurotransmitter detection: towards measuring neurotransmitters as chemical diagnostics for brain disorders, Analytical Methods 11(21) (2019) 2738-2755 DOI: 10.1039/C9AY00055K.

231. E.S. Bucher, R.M. Wightman, Electrochemical analysis of neurotransmitters, Annual review of analytical chemistry 8 (2015) 239-261.

232. C. Owesson-White, A.M. Belle, N.R. Herr, J.L. Peele, P. Gowrishankar, R.M. Carelli, R.M. Wightman, Cue-evoked dopamine release rapidly modulates D2 neurons in the nucleus accumbens during motivated behavior, Journal of Neuroscience 36(22) (2016) 6011-6021.

233. P. Takmakov, C.J. McKinney, R.M. Carelli, R.M. Wightman, Instrumentation for fast-scan cyclic voltammetry combined with electrophysiology for behavioral experiments in freely moving animals, Review of Scientific Instruments 82(7) (2011).

234. E.S. Bucher, K. Brooks, M.D. Verber, R.B. Keithley, C. Owesson-White, S. Carroll, P. Takmakov, C.J. McKinney, R.M. Wightman, Flexible software platform for fast-scan cyclic voltammetry data acquisition and analysis, Analytical chemistry 85(21) (2013) 10344-10353.

235. H. Zhang, S.-C. Lin, M.A. Nicolelis, Spatiotemporal coupling between hippocampal acetylcholine release and theta oscillations in vivo, Journal of Neuroscience 30(40) (2010) 13431-13440.

236. A. Ledo, C.F. Lourenço, J. Laranjinha, G.A. Gerhardt, R.M. Barbosa, Combined in vivo amperometric oximetry and electrophysiology in a single sensor: A tool for epilepsy research, Analytical chemistry 89(22) (2017) 12383-12390.